Signal Integrity Analysis of Transmission Lines in Anisotropic Substrates for High-Speed Data Transmission

by

Srikanth Peddada

A thesis submitted to the Graduate Faculty of
Auburn University
in partial fulfillment of the
requirements for the Degree of
Master of Science

Auburn, Alabama
August 3, 2013

Keywords: Transmission lines, differential pair, anisotropic effects, bit-error-rate contour, signal integrity, phase difference and mode conversion loss.

Approved by

Michael Hamilton, Chair, Assistant Professor, Electrical and Computer Engineering
Michael Baginski, Associate Professor, Electrical and Computer Engineering
Robert Dean, Associate Professor, Electrical and Computer Engineering

Abstract

Continuous increase in high-speed data rates is essential in today's world in order to keep up with Moor's law scaling and to meet application demands. This increase in information transfer rates is essentially limited by the by the inherent characteristics of anisotropic material like printed circuit boards (PCB). One of the limitations is the non-uniformity distribution of resin and fiber in the printed circuit substrate material also known as anisotropic effects. Anisotropic effects introduce differential skew in the signal lines which leads to bit error rate (BER) and limits data rate and length of the transmission lines. It becomes a serious issue for data rates above 3Gbps.

In this thesis, we focus on the anisotropic dielectric properties of PCBs. A solution for reducing phase difference between the differential pair is explored, studied, and simulated on IBIS-AMI models and equalization techniques are applied at the receiver to improve channel performance. Effect of phase difference, length, spread weaves and phase mismatch (isotropic materials) is analyzed to suggest design rules for overall improvement in channel performance.

Acknowledgments

My advisor and committee were the people most directly involved with the completion of my thesis. I would like to express my appreciation and sincere thanks to my advisor Dr. Michael Hamilton, who patiently shaped this work right from the beginning. I benefited greatly from his ability to approach problems from many different directions. I also wish to thank my committee members Dr. Michael Baginski and Dr. Robert Dean for guidance and advise on the work.

I would like to thank my fellow teammates for their support and guidance. And, I would like to thank the committee members for their valuable suggestions and comments.

I am indebted to my parents, sister and all friends for their love and support. I also thank everyone who directly or indirectly helped and inspired me during the course of my graduate study.

Table of Contents

List of Tables

List of Illustrations

1. Introduction

Wired communication refers to transfer of data between transmitter and receiver using physical wires. Physical wires can be internet connection through fiber optic cables or transmitting electronic signal through metal conductor on a printed circuit board (PCB). Advantages of wired communications are reliability, high life expectancy, high speed, quality of service (QoS) and low cost. Maintenance of wired technology is inexpensive and copper has a long life expectancy. Quality of service is excellent because wired communications eliminates the need for establishing end-to-end connection every time. Also the speed of the wired technology is very high, up to 28 Gbps. On the flip side wireless technology suffers from interference and can be un-reliable. Quality of service can be low and wireless communications needs high end wireless equipment that can be costly. Data rates of wireless technology is relatively low, in the range of Mbps. Speed and reliability of wireless lags wired, hence wired technology is useful for transmitting data at high speeds.

Due to it finite conductivity and losses at high frequencies copper wires are being replaced with optical fibers. Fiber optics is a method of transferring data from one place to another by sending pulses of light through optical fiber. Optical fiber has high bandwidths i.e. information can be transmitted at high speeds. Unlike copper wires, no electric current is transmitted down the fiber with which grounding requirements can be and helps it to be immune to electromagnetic interference. Low cost of maintenance and high efficiency puts optical fibers ahead copper wire transmission lines.

The demand for higher data rates and bandwidth has increased day by day. Computers, switches, internet cables and television sets all require higher data rates to meet the increasing demand for media that contains large and large data sizes. Additionally, due to increased demand for number of channels, caused by the increase demand by number of devices/users, the demand for bandwidth is ever increasing. The massive flux of information in and out of chips and systems has caused simple input/output (I/O) drivers to be replaced with sophisticated high-speed circuits which in turn depend on reliable high bandwidth channels. Channel design on PCB boards, which was less important at lower data rates, has become a major concern for high-speed communication. The increase in data rates to the tens of Giga bits per second (Gbps) region has prompted more careful signal integrity considerations in the design of the channel from the transmitter of one chip to the receiver on the next.

This thesis presents an in depth analysis of PCB issues related to high speed passive channels. A technique to mitigate PCB issues for differential pairs and detailed signal integrity analysis for high speed data transmission lines is presented.

2. Literature Survey and Background

Electrical signals are transmitted through metal conductors called transmission lines. Transmission lines are connections capable of carrying signal from transmitter to receiver at high speed. Traditionally, transmission lines have been considered as telecom based cables operating over long distances. But as digital signals are transmitted at high speeds even short traces can be considered transmission lines.

At low frequencies wires are considered to ideal wires without resistance (R) and conductance (G). But at high frequencies as alternating current (AC) dominates transmission line effects will become prominent in the wire. A circuit model of a trace with transmission line effects is shown in Figure 1.
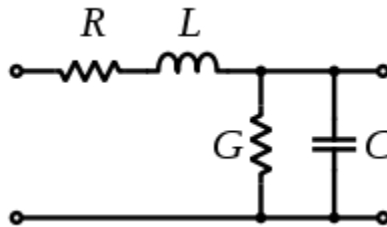
Figure 1. Circuit model of a transmission line [1].

2.1 Characteristics of High speed signals

2.1.1 Return Zero and Non return Zero

The definition of Return-Zero (RZ) logic is if the logic state is a "one", then a pulse of 1/2 the clock period occurs. If the logic state is a "zero", then no pulse occurs, and the signal remains at the

baseline. Obviously, due to its basic pulse nature, an RZ signal has many more transitions compared to NRZ, and less "DC" content.

In Non-Return-Zero (NRZ) a logic "one" is defined as the high voltage state, while a logic "zero" is defined as the low voltage state. Often times, there is also a logic clock signal associated with a logic circuit. Unlike RZ, NRZ does not have a rest state. NRZ is not inherently a self-clocking signal, thus some additional synchronization technique must be used for avoiding bit slip. The binary signal is encoded using rectangular pulse amplitude modulation with return-zero and non-return-zero code is shown in Figure 2.

(a) RZ mode
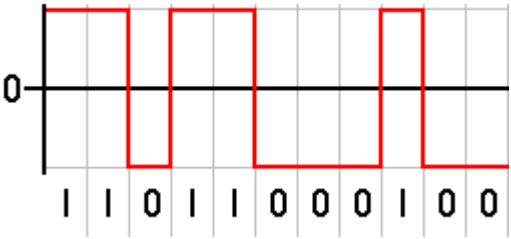
(b) NRZ mode

Figure 2: The binary signal encoded using (a) Return-Zero[2] (b) Non-Return-Zero[3].

2.1.2 Low Voltage Differential Signals (LVDS)

Low-voltage differential signaling is a generic interface standard for high-speed data transmission. In the driver, a current source limits output to

about 3 mA, and a switch box steers the current through the termination resistor. This differential driver produces odd-mode transmission: equal and opposite currents flowing in the transmission lines. The current returns within the wire pair, so the current loop area is small, and therefore generates the lowest amount of EMI (electro-magnetic interference). The current source limits any spike current that could occur during transitions. Because there are no spike currents, data rates as high as 1.5 Gb/s are possible without a substantial increase in power dissipation. In addition, the constant current driver output can tolerate transmission lines shorted together, or to ground, without creating thermal problems.

The differential receiver is a high impedance device that detects differential signals as low as 20 mV and then amplifies them into standard logic levels. The signal has a typical driver offset of 1.2 V, and the receiver accepts an input range of ground to 2.4 V. This allows rejection of common mode noise picked up along interconnect of up to ±1 V. The equivalent circuit structure of the LVDS physical layer is shown in Figure 3.
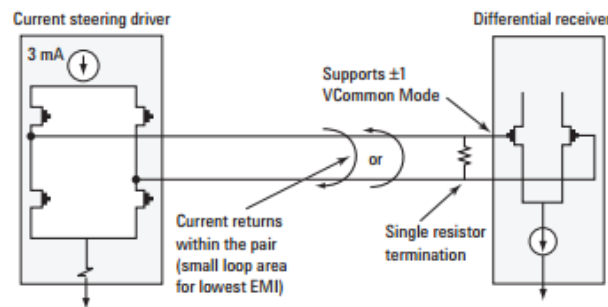
Figure 3. Equivalent circuit structure of the LVDS physical layer [4].

2.1.3 Frequency Spectrum of high speed signals.

As on board frequencies exceed 500 MHz in computer systems, and telecommunications products reach into the 10 Gbps regime, the losses in the circuit board and transmission come into existence.

At low frequencies transmission lines are considered to be lossless. Circuit model for lossless transmission model is shown in Figure 4. As the frequency increases resistance and conductance come into picture as shown in Figure 1 which leads to dielectric losses and conductor losses. These lossy effects result in rise time degradation, added delays, bandwidth reduction and most importantly, pattern dependent noise, often referred to as collapse of the eye diagram.
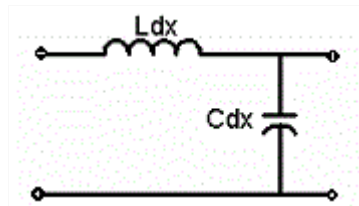
Figure 4. Circuit diagram for lossless transmission lines [1].

The attenuation per length for the model shown in Figure 1 is shown in Equation 1. [6]

$$\alpha = 4.34 * \left(\left(\frac{RL}{Zo} \right) + G_L * Z_o \right) \quad \text{(dB/length)} \qquad (1)$$

Where

α : Attenuation constant.

(R_L/Z_o) : Conductor losses.

(G_L*Z_o): Dielectric losses.

2.1.3.1 Attenuation due to conductor resistance

In the typical case of a 50 ohm transmission line, the attenuation per length due to just the series resistance is given in Equation 2. [6]

$$\alpha_c = 0.09 * R_L \qquad (2)$$

Where

6

α_c : Attenuation due to conductor losses.

At higher frequencies, the inner paths have higher impedance and the outer paths have lower impedance. As frequency increases, there will be a greater tendency for current to take the lower impedance paths, which are toward the outer edge. This is the fundamental origin of skin depth given in Equation 3. [6]

$$\delta = \sqrt{\left[\frac{1}{\pi*\sigma*\mu_o*\mu_r*f}\right]} \qquad (3)$$

Where

δ: Skin depth.

σ: Conductivity of the material.

f: Frequency of the propagating wave.

μ_r: Relative permeability.

As the frequency increases, the cross sectional area available for current flow decreases. This will cause the resistance per length to increase with frequency.

2.1.3.2 Attenuation due to dielectric

When the dielectric completely surrounds the conductors, the attenuation due to just the conductance per length of the dielectric is given by Equation 4. [6]

$$\alpha_d = 2.3 * f * \tan(\delta) * \sqrt{\left[\varepsilon_{eff}\right]} \qquad (4)$$

Where

α_d: Attenuation due to dielectric.

f: Frequency of the propagating wave.

$\tan(\delta)$: loss tangent.

ε_{eff}: effective permittivity.

2.2 Types of transmission lines in Printed circuit board (PCB)

2.2.1 Microstrip transmission line

Microstrip is a type of electrical transmission line which can be fabricated using printed circuit board technology, and is used to convey microwave-frequency signals. It consists of a conducting strip separated from a ground plane by a dielectric layer known as the substrate. Microwave components such as antennas, couplers, filters, power dividers etc. can be formed from microstrip, the entire device existing as the pattern of metallization on the substrate. Microstrip is thus much less expensive than traditional waveguide technology, as well as being far lighter and more compact.

Microstrip lines are also used in high-speed digital PCB designs, where signals need to be routed from one part of the assembly to another with minimal distortion, and avoiding high cross-talk and radiation as shown in Figure 5.
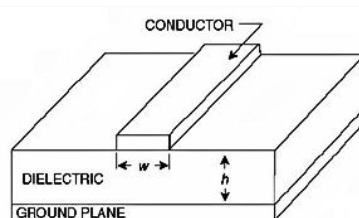
Figure 5. Microstrip transmission line [7].

2.2.2 Stripline transmission line.

A stripline circuit uses a flat strip of metal which is sandwiched between two parallel ground planes. The insulating material of the substrate forms a dielectric as shown in Figure 6. The width of the strip, the thickness of the substrate and the relative permittivity of the substrate determine the characteristic impedance of the strip which is a transmission line.

Stripline is much harder to fabricate than microstrip, and because of the second ground plane, widths are much narrower for a given impedance and board thickness than for microstrip.
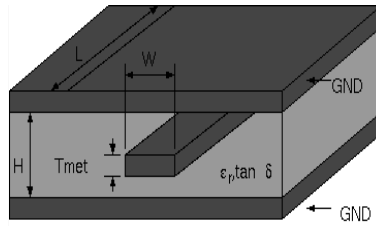
Figure 6. Stripline transmission line. [8]

2.2.3 The Coplanar Waveguide

Coplanar waveguide (CPW) uses a ground conductor that is coplanar with the signal conductor. Therefore, the impedance is controlled by the signal line width and the ground gap. The coplanar waveguide configurations that are most likely to be useful are coplanar waveguide and coplanar waveguide with ground as shown in Figure 7. Coplanar waveguide concentrates the field in the gap so it will have the best ability to taper in to a pin. However, it may require special attention if you are transitioning from microstrip line into CPW. In this situation, coplanar waveguide with ground (CPWG) may be easier to deal with since you can start with a wide gap (microstripline) and gradually transition to the coplanar waveguide with ground configuration.
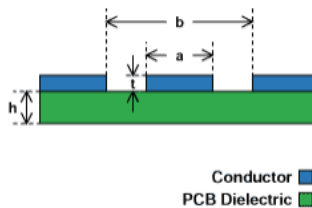
(a) CPW
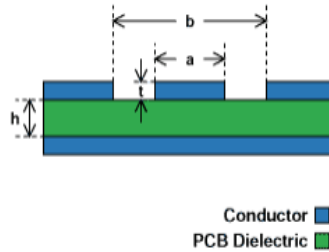
(b) CPWG

Figure 7. Configurations (a) Coplanar Waveguide (b) Coplanar waveguide with ground. [9]

2.2.4 Coaxial Line

The simplest transmission line configuration is coaxial line. It is simple because a there is an exact solution for its impedance and propagation velocity in terms of the physical parameters. There are a couple of places you may want to use the coaxial line in printed circuilar boards.

The first situation is encountered when routing a signal through the printed circuit board. Passing from one layer of the printed-circuit board to another is done with round pads on each layer and holes that are plated with metal to connect these pads. The pad for the via is surrounded by a ground plane. The pad and its surrounding ground plane cut-out form a very short section of coaxial transmission line. You can use coaxial line equations to match these transmission lines to the surrounding circuitry and thus minimize the discontinuity.

Second situation is coaxial lines can provide a fully shielded path for signals on printed-circuit boards in low volume production, as rework, and for prototyping. Coaxial line with inner and outer conductor is shown in Figure 8.
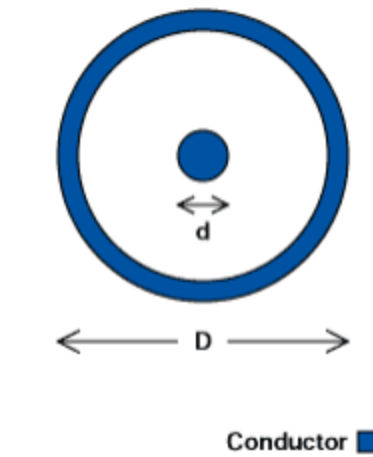
Figure 8: Coaxial line. [9]

2.3 Impedance matching with device impedance

One of the important parameters of the transmission line is characteristic impedance (Zo). In order to maximize the signal transfer we have to design transmission lines whose characteristic impedance is matched with impedance of transmitter and receiver. If the lines are mismatched with the terminal impedance then the signal gets reflected. Multiple reflections can occur within the system, thus reducing the performance of the system. Characteristic impedance of the model shown in Figure 1 is given by the formula [1]

$$Z_o = \sqrt{\left[\left(\frac{R+jwL}{G+jwC}\right)\right]} \qquad (5)$$

In practice we have to design traces with controlled impedance for digital speeds greater than 1 Gbps. If the device impedance is mismatched with impedance of transmitter and receiver multiple reflections will occur in the system and signal is reflected back and forth. This process will continue until all the energy in the signal is absorbed. At high data rates this has detrimental effects on signals and causes effects such as like overshoot, undershoot, ringing and stair step waveform, all of which produce error in signaling. Line impedance is determined by width and

thickness of the conductor, height of the PCB core on either side of the trace, configuration of the lines and dielectric constant of the core. [1]

2.4 Single ended and differential transmission lines

2.4.1 Single ended transmission lines

Single-ended transmission line is probably the most common way to connect devices. In this device driver and receiver are connected by a single conductor as shown in Figure 9. For single-ended transmission lines, a reference plane (ground planes) provides the current return paths.
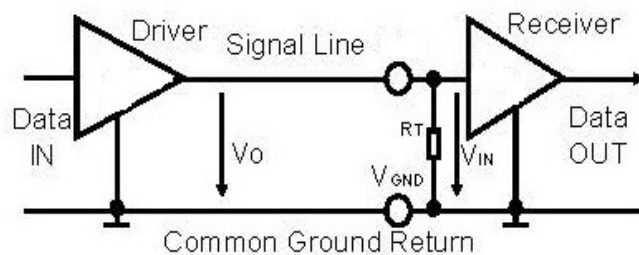
Figure 9. Single-ended transmission line. [10]

The signal and return lines differ in geometry — the cross-section of the signal conductor is different from that of the return ground plane conductor. Characteristic impedance of the single-ended transmission line is determined by width and thickness of the conductor, height of the dielectric and dielectric constant of the system. The number of conductors used in a complex design will be less when compared to a system that uses differential pairs, however the receiver receives noise signal with respect to ground planes.

2.4.2 Differential transmission lines

Differential transmission lines are driven as a pair with one line transmitting the signal waveform of the opposite polarity (180°) to other as shown in Figure 10.
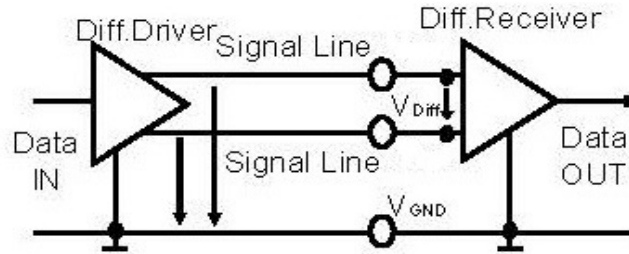
Figure 10. Differential transmission lines. [10]

Characteristic impedance of the differential pair is determined by width, thickness and spacing of the conductor, height of the dielectric medium and dielectric constant of the medium. The number of conductors will be more when compared with single ended but common mode noise, generated in the two lines will tend to cancel out and EMI will be lower in the differential lines therefore problems with noise will be reduced.

2.4.3 Advantages of differential over single ended transmission lines

Differential lines reduce electronic crosstalk and electromagnetic interference. Owing to the ability of noise rejection, signal swing can less in differential signaling when compared to single ended, which can result in lower power systems at higher data rates.

2.5 Definitions

2.5.1 S-parameters

S-parameters (or scattering parameters) describe the electrical behavior of electrical networks when undergoing various steady state changes by electrical signals [11]. Many electrical properties of components like resistance, inductance, and capacitance can be captured using S-parameters such as gain, return loss, insertion loss, and voltage standing wave ratio and reflection coefficient. S-parameters are generally expressed as complex numbers either in rectangular form or polar form. An electrical network may have N number of ports. Ports are the points where the signal enter or exits the system.

2.5.2 Even mode

In even mode signals are driven with equal in magnitude and phase i.e. currents in the differential pair are propagating **same** direction. Electric fields and magnetic fields for even mode are shown in Figure 11.
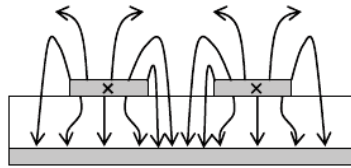
(a) Electric Field
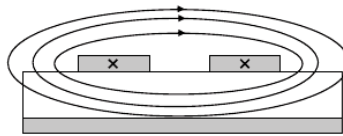
(b) Magnetic Field

Figure 11. (a) Electric field (b) Magnetic field for even mode. [18]

   Current into the page

   Current out of the

For Figure 10 if,

Z_{o1}- Characteristic impedance of trace 1.

Z_{o2}- Characteristic impedance of trace 2.

then even mode impedance is the twice the common mode impedance.

$$Zc = \frac{Z01 + Z02}{2}$$ (6)

2.5.3 Odd mode

In even mode signals are driven with equal in magnitude and 180° out of phase i.e. currents in the differential pair propagate in opposite direction. Electric fields and magnetic fields for even mode are shown in Figure 12.

(a) Electric field
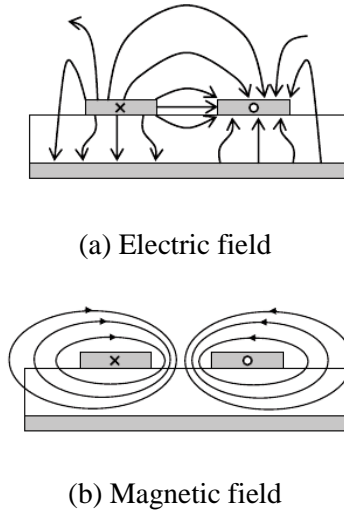
(b) Magnetic field

Figure 12. (a) Electric field (b) Magnetic field for odd mode. [18]

Current into the page

Current out of the

For Figure 10 if,

Z_{o1}- Characteristic impedance of trace 1.

Z_{o2}- Characteristic impedance of trace 2.

then odd mode impedance is the twice the differential impedance.

$$Z_0 = 2*(Z_{o1} - Z_{o2}) \qquad (7)$$

In differential pair even mode and odd mode currents exists and it can be analyzed by using mixed mode S-parameters.

15

2.5.4 Two-port network model

A two-port network is an electrical network with two pairs of terminals to connect to external circuits. Ports constitute the interface between the input network and other networks. Signal enters through input port and exit through output port. Two-port network is shown in Figure 13 with port 1 as input port and port2 as output port.
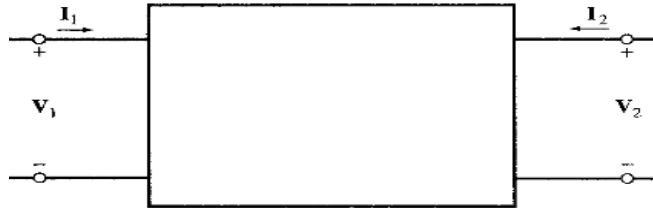
Figure 13. Two-port network model.

V_1, I_1 – Input voltage and current.

V_2, I_2- Output voltage and current.

2.5.4.1 Two-port S-parameters

S-parameter matrix for two-port network will be a 2X2 square matrix with 4 elements. Two-port networks with reflected and incident power wave are shown in Figure 14.
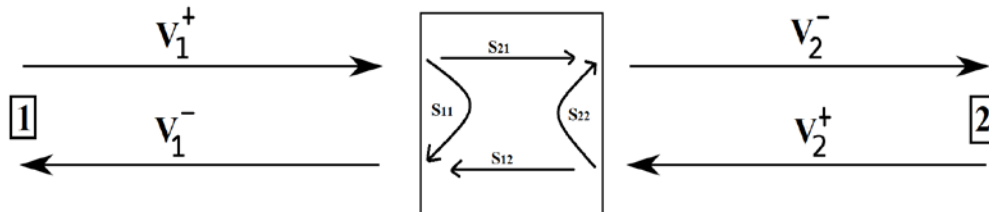
Figure 14. Two-port S-parameter network model. [12]

For a matched load S-parameters for two-port network is given by

$S_{11} = \frac{V1^-}{V1^+}$

$S_{12} = \frac{V1^-}{V2^+}$

$S_{21} = \frac{V2^-}{V1^+}$

$S_{22} = \dfrac{V2^-}{V2^+}$

Where S_{11} = Input port voltage reflection coefficient.

S_{12} = Reverse transmission coefficient.

S_{21} = Forward transmission coefficient.

S_{22} = Output port voltage reflection coefficient.

2.5.5 Mixed mode S-parameters

Digital systems continue to gain in speed, well beyond 1 Gb/s, requiring new methods of analysis and testing. Traditional S-parameters are useful when working with single ended devices. But mixed-mode S-parameters provide the capability of analyzing and visualizing the signal flow through differential (balanced) lines and devices found in modern high-speed digital communications systems.

Mixed mode S-parameters refers to the point that trace signals have even mode and odd mode components. In differential mode a non-zero potential exists between the differential pair and in common mode combined the traces, a non-zero potential exists between the traces and ground as shown in Figure 15.

Figure 15. Differential mode and common mode. [19]

After performing simulations for the design shown in Figure 15 we get S-parameters matrix of 4X4 size as shown in Equation 6

$$\begin{bmatrix} S_{11} & S_{12} & S_{13} & S_{14} \\ S_{21} & S_{22} & S_{23} & S_{24} \\ S_{31} & S_{32} & S_{33} & S_{34} \\ S_{41} & S_{42} & S_{43} & S_{44} \end{bmatrix} \tag{8}$$

After performing linear transformation mixed mode parameter shown in Equation 7.

$$\begin{bmatrix} S_{d1d1} & S_{d1d2} & S_{d1c1} & S_{d1c2} \\ S_{d2d1} & S_{d2d2} & S_{d2c1} & S_{d2d2} \\ S_{c1d1} & S_{d1c2} & S_{c1c1} & S_{c1c2} \\ S_{d2c1} & S_{d2c2} & S_{c2c1} & S_{c2c2} \end{bmatrix} \tag{9}$$

Where

d1: differential combination of port 1 and port 2

d2: differential combination of port 3 and port 4

c1: common combination of port 1 and port 2

c2: common combination of port 3 and port 4

2.5.5.1 Differential to Differential parameters: S$_{DD}$

Differential to differential parameters are similar to single-ended S-parameters but specific to odd-mode propagation of signal. Generally of most interest in characterizing differential signals in the device as shown in Figure 16. Poor S$_{DD}$ performance results in direct degradation in bit error rate and attainable data rate or bandwidth.

Figure 16. Differential to differential mode. [19]

18

2.5.5.2 Common to Differential parameters: S_{DC}

Common to differential parameters measures susceptibility to noise from outside sources. These parameters arises due to imbalance between true and complement traces. Poor S_{DC} performance can result in outside noise affecting differential signal performance. Note the convention used in naming common to differential parameters (S_{DC}). Common to differential mode design is shown in Figure 17.

Figure 17. Common to differential mode. [19]

2.5.5.3 Differential to Common parameters: S_{CD}

Differential to common parameters measure signal emission to outside environment. Poor S_{CD} performance can result in generation of unwanted noise coupling into other interconnect. Differential to common mode is shown in Figure 18.

Figure 18. Differential to common mode. [19]

2.5.5.4 Common to Common parameters: S_{CC}

Common to common parameters are similar to single-ended S-parameters but specific to even-mode propagation of signal. Poor S_{CC} performance can result in common-mode shifts in signals and ground/supply-loop currents. Common to common mode is shown in Figure 19.

Figure 19. Common to common mode. [19]

2.5.6 Conversion from Single ended to mixed mode S-parameters.

Through variable substitution and carrying through the math, we can now obtain the relationship between single-ended and mixed-mode S-parameters.

2.5.6.1 Differential to Differential parameters

Differential to differential parameters from single ended parameters are given in Equation 10. [19]

$$
\begin{aligned}
S_{D1D1} &= \frac{1}{2}\left(S_{11} - S_{21} - S_{12} + S_{22}\right) \\
S_{D1D2} &= \frac{1}{2}\left(S_{13} - S_{23} - S_{14} + S_{24}\right) \\
S_{D2D1} &= \frac{1}{2}\left(S_{31} - S_{41} - S_{32} + S_{42}\right) \\
S_{D2D2} &= \frac{1}{2}\left(S_{33} - S_{43} - S_{34} + S_{44}\right)
\end{aligned}
\tag{10}
$$

2.5.6.2 Differential to common parameters

Differential to common parameters from single ended parameters are given in Equation 11. [19]

$$
\begin{aligned}
S_{C1D1} &= \frac{1}{2}\left(S_{11} + S_{21} - S_{12} - S_{22}\right) \\
S_{C1D2} &= \frac{1}{2}\left(S_{13} + S_{23} - S_{14} - S_{24}\right) \\
S_{C2D1} &= \frac{1}{2}\left(S_{31} + S_{41} - S_{32} - S_{42}\right) \\
S_{C2D2} &= \frac{1}{2}\left(S_{33} + S_{43} - S_{34} - S_{44}\right)
\end{aligned}
\tag{11}
$$

2.5.6.3 Common to differential parameters

Common to differential parameters from single ended parameters are given in Equation 12. [19]

$$
\begin{aligned}
S_{D1C1} &= \frac{1}{2}\left(S_{11} - S_{21} + S_{12} - S_{22}\right) \\
S_{D1C2} &= \frac{1}{2}\left(S_{13} - S_{23} + S_{14} - S_{24}\right) \\
S_{D2C1} &= \frac{1}{2}\left(S_{31} - S_{41} + S_{32} - S_{42}\right) \\
S_{D2C2} &= \frac{1}{2}\left(S_{33} - S_{43} + S_{34} - S_{44}\right)
\end{aligned}
\tag{12}
$$

2.5.6.4 Common to common parameters

Common to common parameters from single ended parameters are given in Equation 13. [19]

$$
\begin{aligned}
S_{C1C1} &= \frac{1}{2}\left(S_{11} + S_{21} + S_{12} + S_{22}\right) \\
S_{C1C2} &= \frac{1}{2}\left(S_{13} + S_{23} + S_{14} + S_{24}\right) \\
S_{C2C1} &= \frac{1}{2}\left(S_{31} + S_{41} + S_{32} + S_{42}\right) \\
S_{C2C2} &= \frac{1}{2}\left(S_{33} + S_{43} + S_{34} + S_{44}\right)
\end{aligned}
\tag{13}
$$

In this thesis, analysis will be based on differential to differential Reflection loss (S_{d1d1}), differential to differential Insertion loss (S_{d2d1}) and differential to common mode conversion (S_{c2d1}).

2.5.7 Insertion loss and return loss. [12]

2.5.7.1 Insertion loss

Insertion loss is the extra loss produced by the network present between the ports and is expressed in decibels. Insertion loss is a measurement of forward transmission coefficient.

$$IL = -20*\log (S_{21}) \text{ dB} \tag{14}$$

For maximum signal transfer forward transmission coefficient should be high and insertion loss should be close to 0 dB

2.5.7.2 Return loss

If the system impedance does not match with terminal impedance then signal gets reflected at the input terminal and output terminal. Return loss (RL) is expressed in terms of decibels and is a measure of input port reflection coefficient.

$$RL = -20*\log (S_{11}) \text{ dB} \tag{15}$$

For maximum transfer of signal reflections at the input port should be low and return loss should be below -30 dB, as a rule of thumb.

2.5.8 Eye diagram

An eye diagram is a useful tool for the analysis of signal used in digital transmission. It provides at-a-glance evaluation of system performance and can offer insight into the nature of channel imperfections. An ideal eye diagram and eye diagram with imperfections are shown in Figure 20

(a)

22
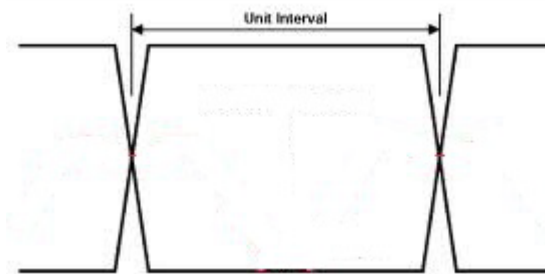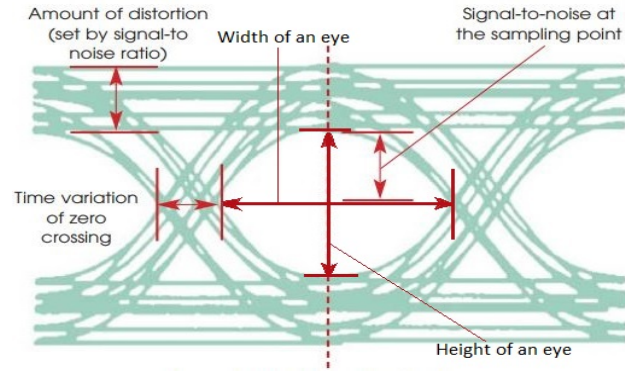
(b)

Figure 20 (a) Ideal eye diagram. (b) Eye diagram with imperfections [13].

In our analysis, an important factor to consider is the area of the eye diagram which is the product of height and width of an eye. As bit rate increases due to differential skew and signal to noise ratio, area of the eye diagram decreases. In order to increase the area of eye diagram we apply equalization techniques.

2.5.9 Differential skew and Bit-error-rate (BER)

2.5.9.1 Differential skew

Differential skew has become a fundamental limiting factor for high speed data transmission lines. Differential skew refers to length or time difference between the differential pair. Differential skew limits the band width of these links, adds jitter and limits the optimization to compensate losses in differential pair [14].

Differential skew arises from a variety of sources. The most common and universal cause of skew is difference in electrical length of the transmission lines. Differential skew affects the width of an eye diagram. Complex structures shown always experiences differential skew and can be resolved by matching the length of transmission lines as shown in Figure 21.

23
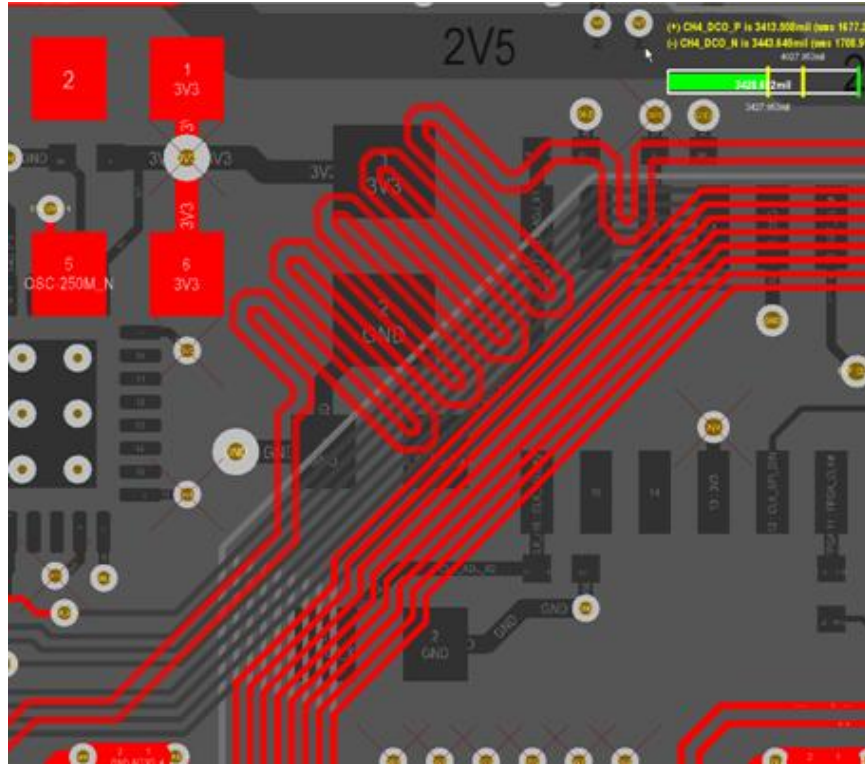
Figure 21: Skew elimination by length matching [15].

2.5.9.2 Bit-error-rate (BER) and BER Contours

Bit error rate (BER) is the number of bit errors divided by the total number of transferred bits during a studied time interval. Most communication links are ultimately judged by their Bit Error Rate (BER) performance or how many bits arrive at their destination in error [14].

A method of viewing link performance that is intuitive, but that contains all of the information needed to judge real link performance would be useful. Therefore engineers are increasingly turning to BER contour as a powerful indicator. BER contours fall inside the visible representation of the eye. At the receiver if we define BER contours to be 10^{-13}, 10^{-12} and 10^{-11}, then outer most contours shown in Figure 22 represents 10^{-13} BER contour and it indicates 10^{-13} bit falling inside the contour is free from errors.

24

Figure 22. BER contours [14].

As the channel performance decreases BER contours closes. Equalization techniques at the transmitter and receiver are applied to open BER contours.

2.6 Equalization techniques

An ideal transmission line can transmit a signal without any loss or distortion. In reality signal gets distorted as it reaches receiver due to factors like loss, noise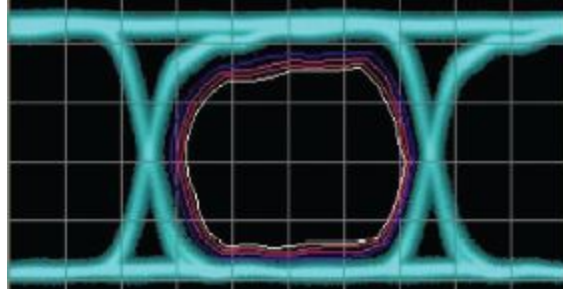, jitter etc. Equalization techniques are proposed by the engineers to improve the signal at the output. Transmitter Feed Forward Equalization (TX FFE) at the transmitter pre-distorts the transmitter pulse in order to invert channel distortion. At receiver we have Receiver Feed Forward Equalizer (RX FFE), Decision Feedback Equalization (DFE) and Continuous Time Linear Equalizer (CTLE) which can be implemented as part of the receiver circuit and flattens the system response through conditioning the received signal. Equalization techniques for transmitter and receiver are shown in Figure 23.
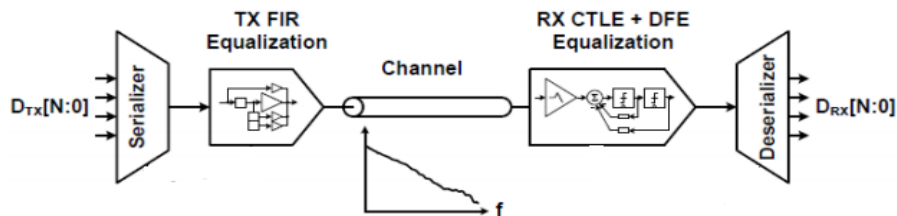
Figure 23. Transmitter and receiver with Equalization settings. [26]

2.6.1 TX Feed Forward Equalization (TX FFE)

Transmitter equalization technique is the most common technique in high speed links design; it is usually implemented through FIR filter. TX FFE pre-distorts the data over several bit periods in order to invert the channel distortion. This can be explained from an example. Without equalization, a transmitter

transmits single pulse as the red curve shown in Figure 24(a). The pulse gets distorted by a channel as the

red curve shown in Figure 24(b). By using FFE the pulse is reshaped as the blue curve shown in Figure

24(a). The pulses at time -1 and 1 ns are generated to cancel the channel`s pulse response. The equalized

pulse is shown as the blue curve in Figure 24(b). Tap coefficients and improved response of the system

using TX FFE is shown in Figure 24(c), 24(d).

(a)

(b)

(c)

Channel Response w/ TX FIR Eq
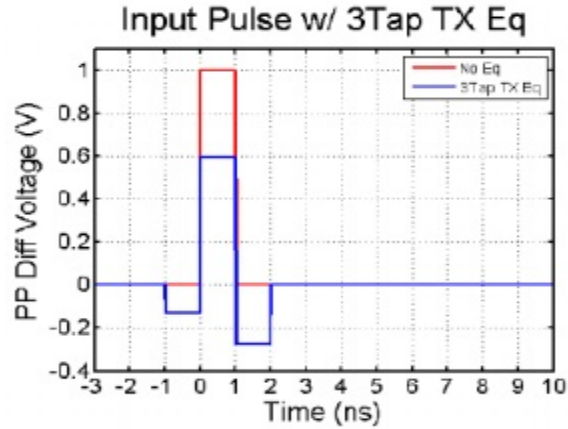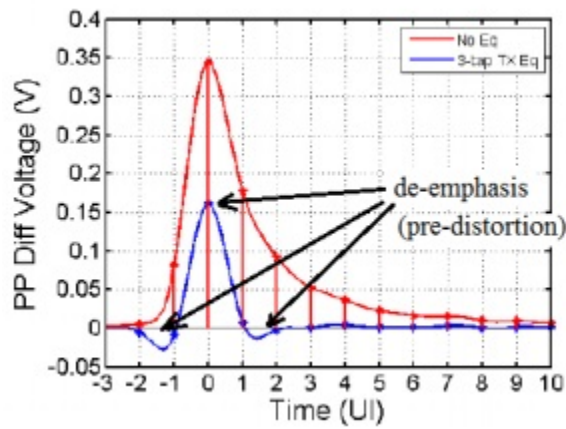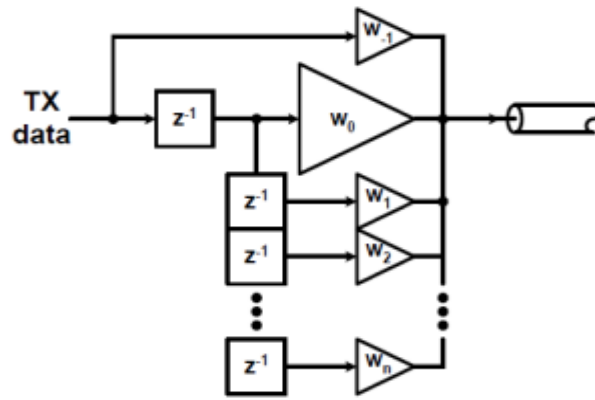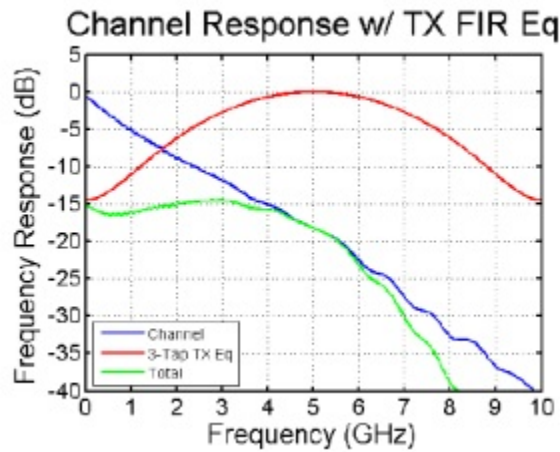
(d)

Figure 24. (a) Input pulse with 3 tap TX Equalization (b) Pulse received at the receiver with and without equalization (c) TX Equalization with filter (d) Frequency response with and without equalization. [24]

Figure 24(d) shows frequency response of the device with and without equalization. Without equalization there will be reflections at lower frequencies and after equalization amount of reflection at the transmitter is reduced considerably.

2.6.1.1 Advantages and disadvantages [24]**.**

Advantages:

- TX FFE can cancel pre-cursor ISI.

- Due to the digital nature of the TX FFE, the noise is not amplified.

27

- 5-6 bit resolution can be achieved.

  Disadvantage:

- To flatten the channel response, low frequency content is attenuated due to the peak power limitation.

2.6.2 RX Feed Forward Equalization (RX FFE)

RX feed forward equalizer at the receiver can be realized as shown in Figure 25. As the receiver signal contains channel response information, filter tap coefficients can be adaptively tuned. As the signal pass through RX FIR depending on the gain and tap coefficients waveforms are generated at every tap setting. Waveforms at every tap settings are added to produce an equalized waveform.
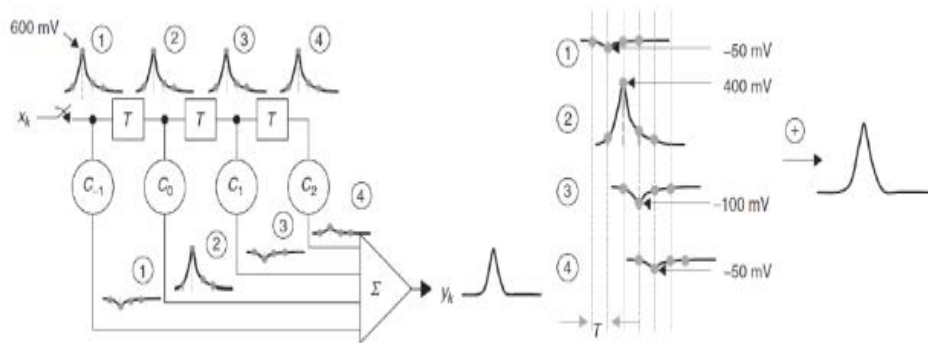
Figure 25. RX FFE Equalization [24]

2.6.2.1 Advantages and disadvantages [24]

Advantages:

- Amplify high frequency content rather than attenuate low frequency components.

- Filter tap can be adaptively tuned.

  Disadvantages:

- Noise and crosstalk are amplified at the same time.

- Tap precision is difficult to meet.

2.6.3 RX Continuous Time Linear Equalizer (CTLE)

Both linear passive and active filter can realize high-pass transfer function to compensate

for channel loss as shown in Figure 26.
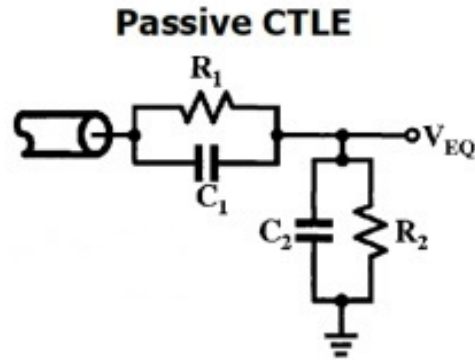
(a)
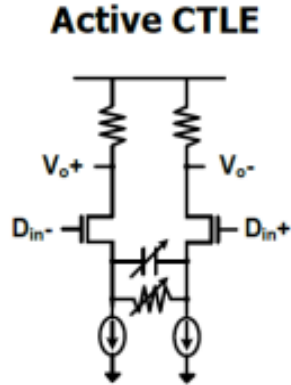
(b)

Figure 26. (a) Passive filter (b) Active filter. [25]

The passive CTLE is the combination of passive low pass filter and high pass filter. The transfer

function of Passive CTLE shown in Figure 26 (a) is given in equation 16.[25]

$$H(S) = \frac{R_2}{R_1 + R_2} \frac{1 + R_1 C_1 S}{1 + \frac{R_1 R_2}{R_1 + R_2}(C_1 + C_2)} \qquad (16)$$

At DC, the capacitors can be ignored and the filter becomes a resistor divider circuit. DC gain is given in Equation 17. [25]

$$DC\ gain = \frac{R_2}{R_1 + R_2} \qquad (17)$$

At AC, the capacitors become low impedance elements. The AC gain is determined by capacitors. AC gain is given in Equation 18.[25]

$$AC\ gain = \frac{C_1}{C_1 + C_2} \qquad (18)$$

Transfer function for the active filter is given in Equation 19.[25]

$$H(s) = \frac{gm}{Cp} \frac{s + \frac{1}{RsCs}}{\left(s + \frac{1 + gmRs/2}{RsCs}\right)\left(s + \frac{1}{RdCp}\right)} \qquad (19)$$

DC gain for the active filter is given in Equation 20[25]

$$DC\ gain = \frac{gmR_D}{1 + gmR_s/2} \qquad (20)$$

2.6.3.1 Advantages and disadvantages [25]

Advantage

- Active CTLE provides gain and equalization with low power and area overhead.

Disadvantages

- Equalization is limited to 1st order compensation.

- Noise and cross talk are amplified

- The speed is limited by gain bandwidth of the amplifier.

2.6.4 RX Decision Feedback Equalizer

Decision feedback equalizer is commonly implemented in high-speed inks receiver-side. Slicer makes a symbol decision without amplifying noise. The results are fed back to the slicer input through an FIR filter. The major challenge in DFE implementation is the closing timing on the first tap feedback, which must be done in one bit period or one unit interval (UI). RX DFE is shown in Figure 27

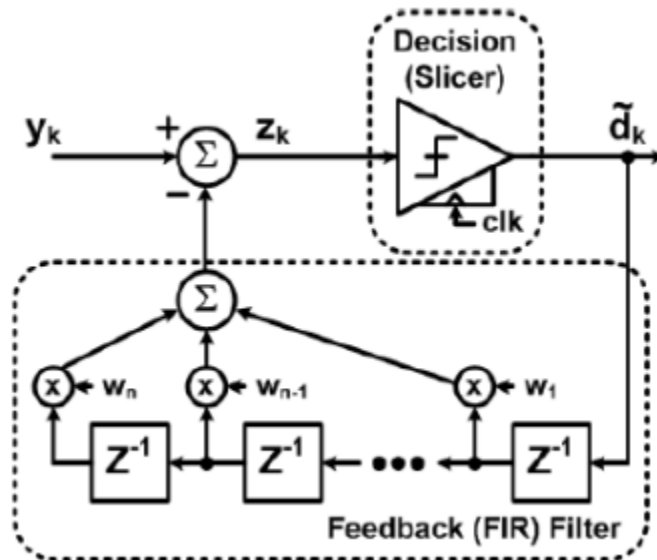Figure 27. RX Decision Feedback Equalizer. [16]

2.6.4.1 Advantages and disadvantages [16]

Advantages

- Boost high frequency content without noise and crosstalk amplification.

- Tap coefficients can be adaptively tuned.

Disadvantages

31

- If noise is large, chance for error propagation is high.

- Critical feedback timing path is less than one UI.

2.7 Transmitter and Receiver AMI models.

2.7.1 Introduction to AMI

AMI (Algorithmic Modeling Interface) is the modeling interface for SERDES (a pair of Serializer and Deserializer) behavioral models which simulate SERDES functionalities such as equalization. AMI is introduced as an extension to the IBIS (Input Output Buffer Information Specification) standard. The AMI portion is specified in IBIS file as part of the IBIS model. An AMI model acts as a DSP block which takes an input signal waveform and outputs a modified waveform.

2.7.2 AMI model files

AMI model consists of the following files:

- .ibs file: specifies file names and compilation platform.

- .ami parameter file: specifies model parameters.

- DLL (.dll) or shared object (.so) file: three functions:

2.7.3 AMI Parameter

These are following types of AMI parameters

Reserved: Reserved parameters are common parameters shared by all models. Their names, types and meanings are defined by the AMI standard.

Model Specified: Model specific parameters are private to the model. Model makers can define any number of model specific parameters under any name and any type.

The AMI methodology divides the channel system into three parts:
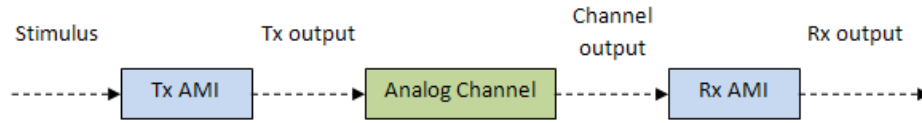
- Tx AMI block.

- Analog channel.

- Rx AMI block.

Figure 28. AMI methodology. [20]
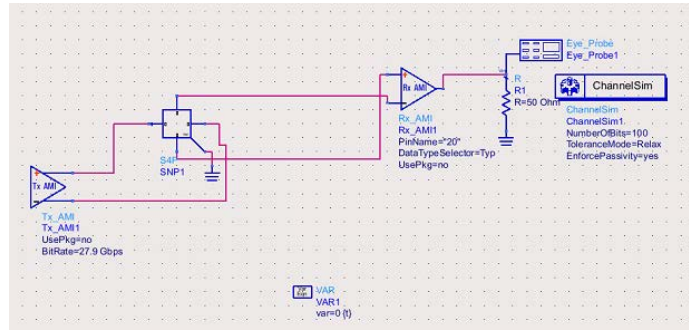
Figure 29. Design level implementation of AMI methodology.

3. Fiber weaves effects of anisotropic materials

3.1 Introduction

Transmission lines that link transmitter and receiver are limited by the inherent characteristics of anisotropic material like printed circuit boards (PCB). One of the limitations is the non-uniformity distribution of resin and fiber in the printed circuit substrate material also known as fiber weave effect (FWE). Fiber weave effects introduce differential skew in the signal lines which leads to bit error rate and limits data rate and length of the transmission lines.

3.2 Fiber weave effect (FWE)

Fiber weave effect limits the performance of the channel and poses signal integrity issues due to difference in dielectric constant of the PCB substrate. It becomes a serious issue for data rates above 3Gbps.

Printed circuit boards are made up of two types of materials: fiber ($\varepsilon_r \approx 4.4$) and resin ($\varepsilon_r \approx 3.3$). Fiber forms the strength of the board and is woven like any other normal weave and the gaps are filled with resin. The speed at which signal propagates depends on material relative permeability. Variation of dielectric constant due to laminate weave is shown in Figure 30.
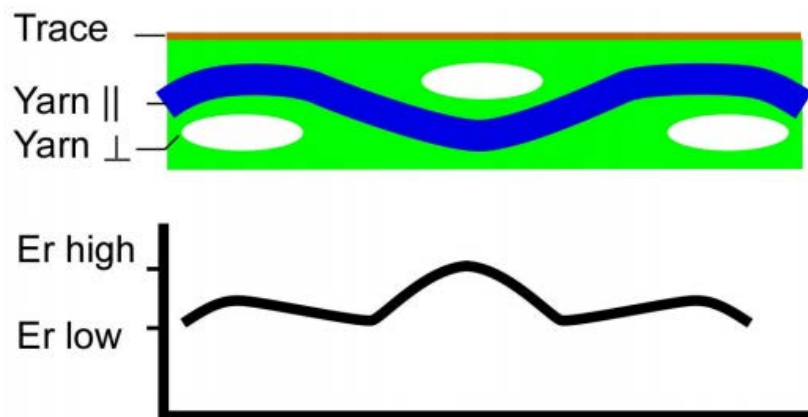
Figure 30. ε_r variation due to laminate weave [21]

34

The speed with which signal propagates depends on dielectric constant. The higher the dielectric, the slower the signal propagates with in the transmission line. Knowing the dielectric constant propagation delay can be found out using Equation 21. [27]

$$T_{pd} = \frac{\sqrt{\varepsilon_r}}{c}$$ (21)

Where:

T_{pd} = Propagation delay.

ε_r= relative permeability or dielectric constant.

c= speed of light (3×10^8m/sec).

At greater speeds this problem will become significant and poses limitation in terms of data rate and length of the transmission lines.

3.3 Typical laminate weaves

Typical PCB dielectric substrates are constructed from various woven fiberglass fabrics strengthened and bound together with epoxy resin. Figure 31 shows typical laminate weaves. The numbers with which each laminate weave is named identify the glass fabric style based on the fiberglass thickness, pitch, warp yarn, fill yarn, and the number of glass fiber strands used.
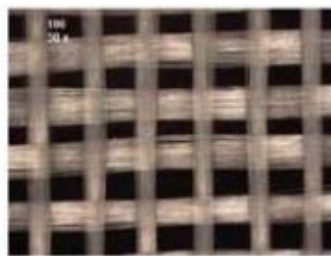
(a) 106 laminate weave
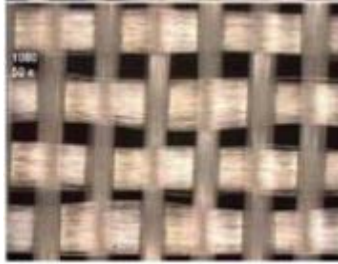
(b) 1080 laminate weave
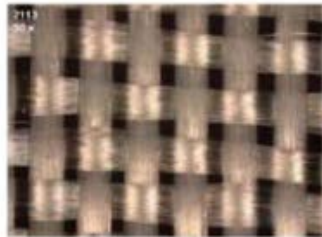
(c) 2113 laminate weave.
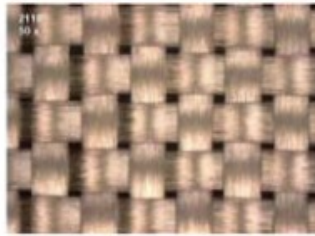
(d) 2116 laminate weave
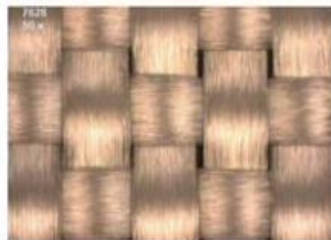
(e) 7628 laminate weave

Figure 31 (a) 106 laminate weave (b) 1080 laminate weave (c) 2113 laminate weave (d) 2116 laminate weave (e) 7628 laminate weave [22]

3.4 Solution to fiber weaves effect

A solution to mitigate the effects of fiber weaves is proposed. Transmission lines mounted on the printed circuit board are rotated from 0 degrees to 45 degrees to average out of the effects of anisotropic. S-parameters are extracted for each angle of rotation and inserted into a 4-port network model and equalization techniques are applied to optimize the channel performance.

Another solution to mitigate the effects of anisotropic is use of tight/spread weaves. Traditional fabrics (106, 1080) are loosely woven fabrics with resin filling the gaps and this affects the signal propagation. In case of tight/spread weaves (7628) shown in Figure 31 fibers are closely spaced leaving small pores filled with resin, this will have very less effect on signal propagation.

4. Channel performance

Signal integrity analyses were performed on anisotropic substrate. High Frequency Simulator software (HFSS) and Advanced Design Systems (ADS) software are used to perform the simulations.

4.1 Fiber and resin

To begin the analyses, I have designed a basic model in which the substrate is divided into two parts fiber and resin as shown in Figure 32 to observe the effects of dielectric constant on the differential pair.
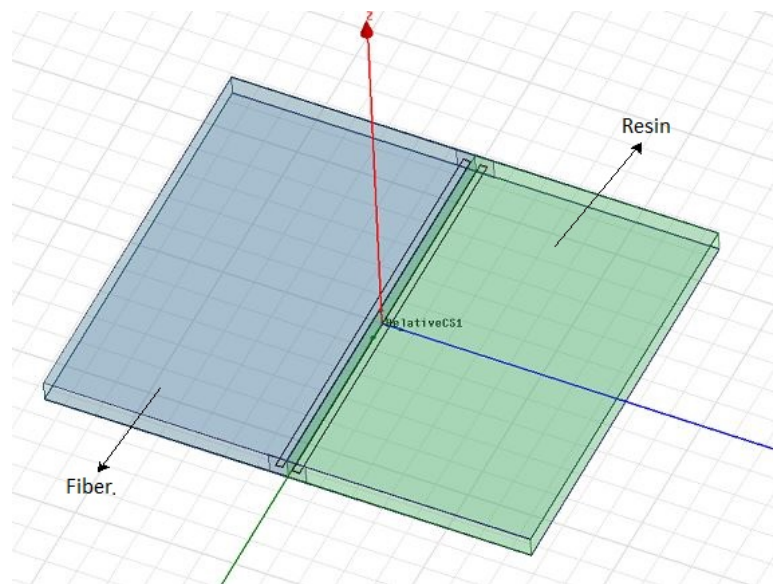
Figure 32. Fiber and resin design

Specifications for the design shown in Figure 32 are

- Width: 4.63 mils

- Spacing: 5.8 mils

- Length: 0.25in

- Dielectric constant for resin: 3.3

- Dielectric constant for fiber: 4.4

Now the differential pair is rotated from 0 degree to 90 degree angle of rotation as shown in

Figure 33.
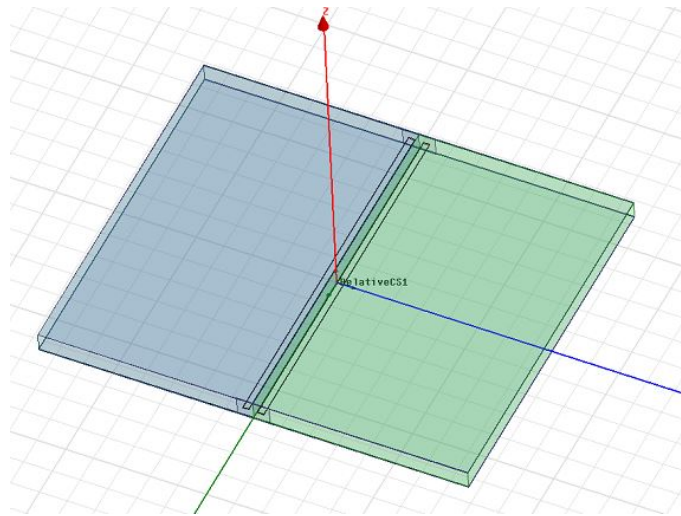
(a) Zero degree rotation
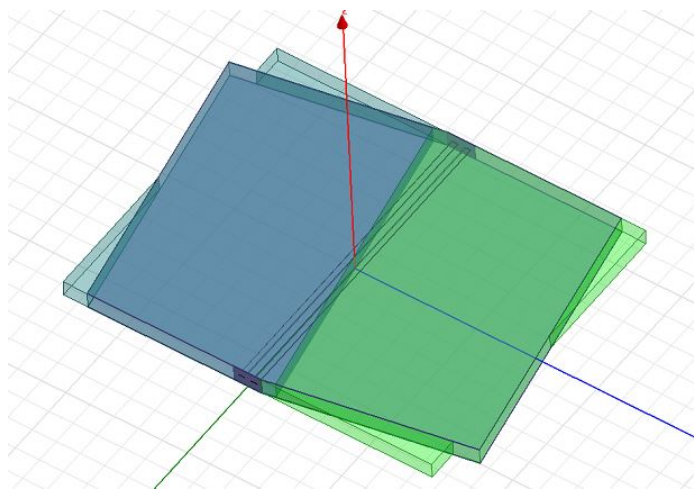
(b) 10 degree rotation
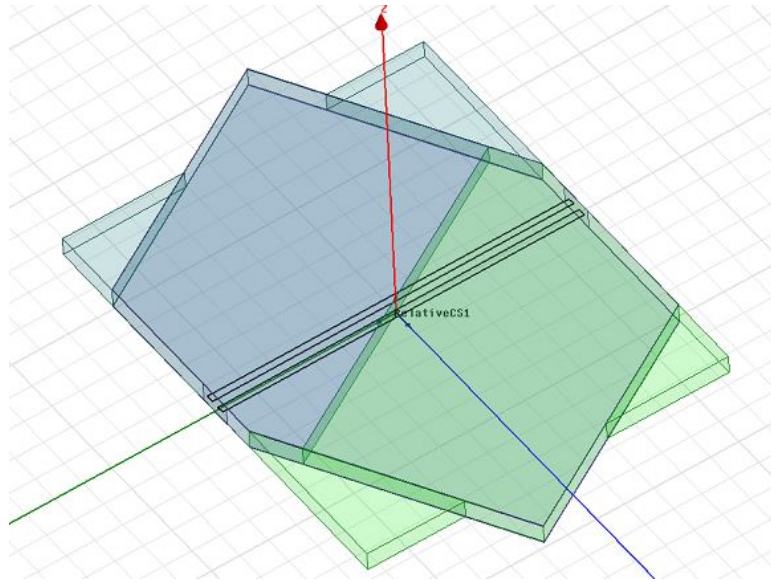
(c) 30 degree rotation
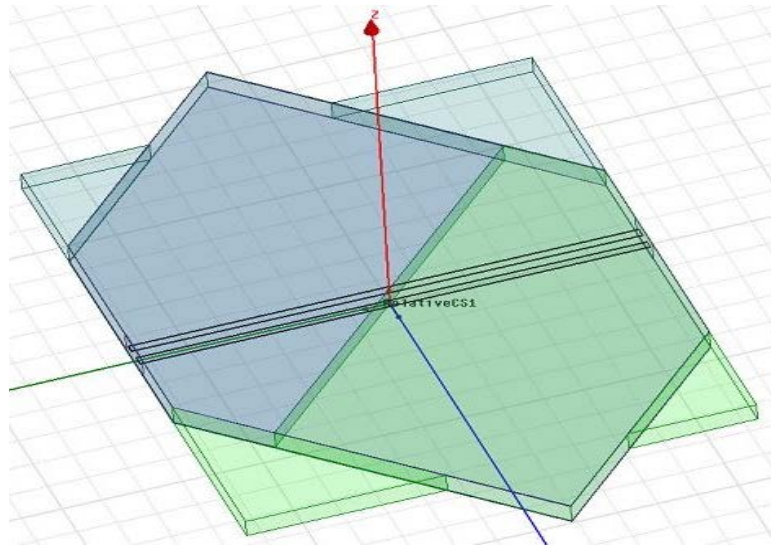
(d) 45 degree rotation
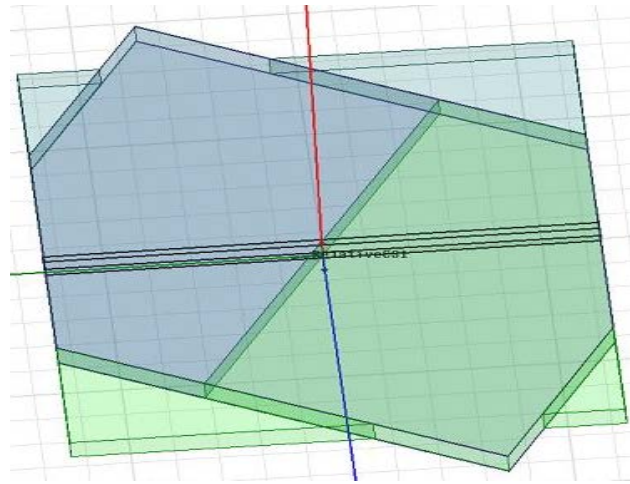
(e) 60 degree rotation
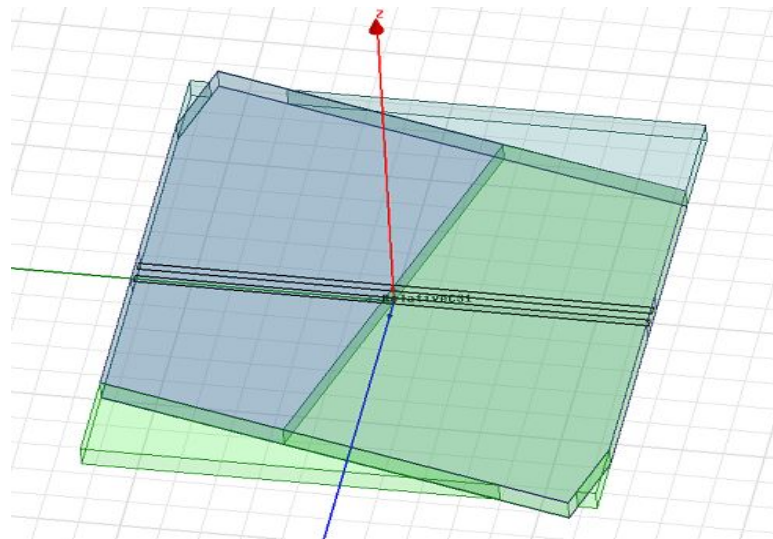
(f) 75 degree rotation
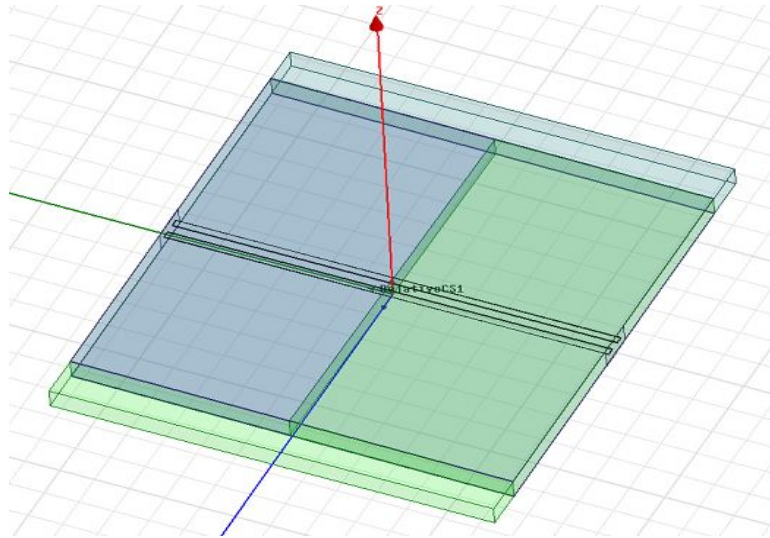
(g) 90 degree rotation

Figure 33. Fiber and resin (a) Zero degree (b) 10 degree (c) 30 degree (d) 45 degree (e)

60 degree (f) 75 degree (g) 90 degree rotation angle of rotation.

As mentioned earlier in chapter 3.2 due to change in dielectric constant signal in the differential pair travels with different speeds resulting in differential skew. This phenomenon can be seen in Figure 34(a).

Phase angle plots for each angle of rotation are shown in Figure 34.

(a) Zero degree rotation

(b) 10 degree rotation

(c) 30 degree rotation

(d) 45 degree rotation

43
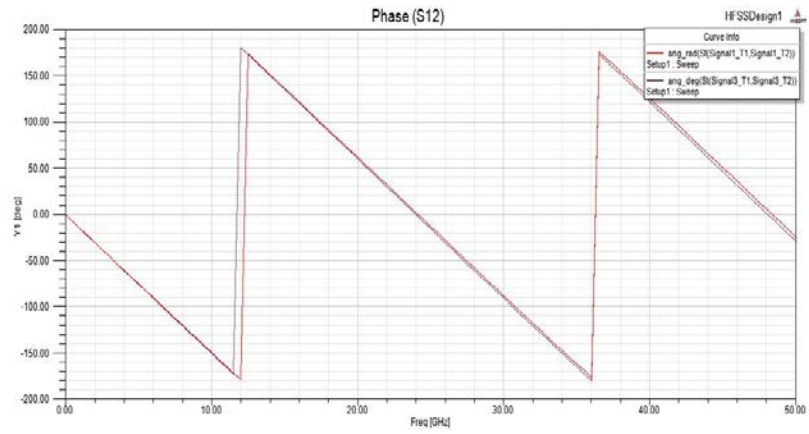
(e) 60 degree rotation

(f) 75 degree rotation

(g) 90 degree rotation

Figure 34. Phase angle plots for (a) zero degree (b) 10 degree (c) 30 degree (d) 45 degree (e) 60 degree (f) 75 degree (g) 90 degree angle of rotation.

Differential to differential return loss (S_{d1d1}), differential to differential insertion loss (S_{d2d1}) and differential to common mode conversion loss (S_{c2d1}) and phase difference plots for each angle of rotation are shown in Figure 35.
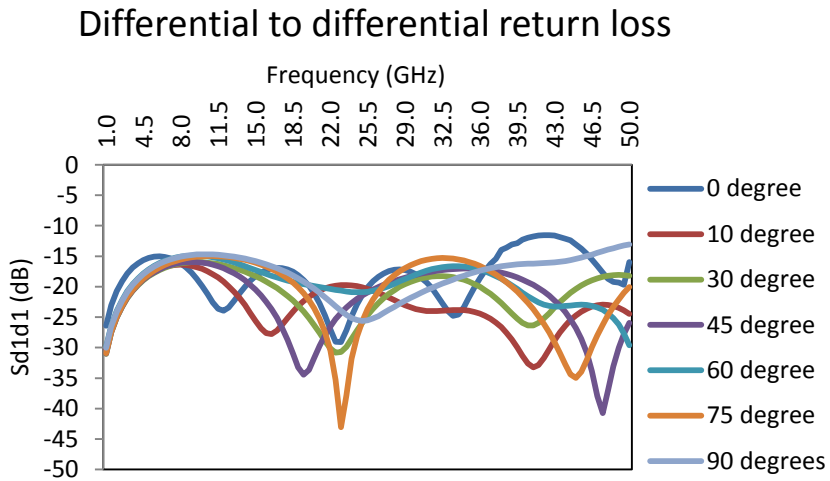
(a) Differential to differential return loss.

Differential to differential insertion loss
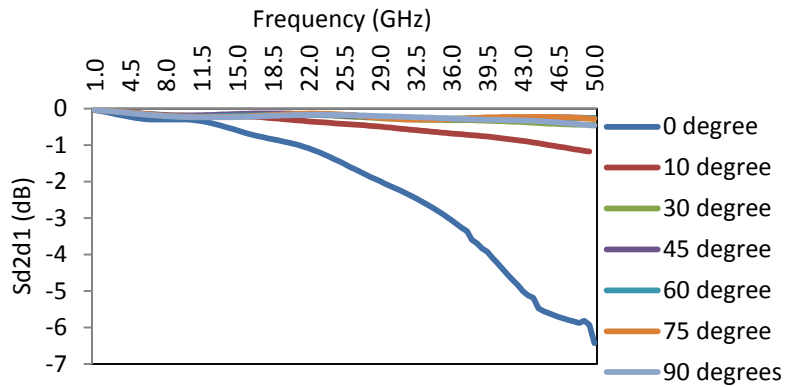
(b) Differential to differential insertion loss.

Differential to common mode conversion loss
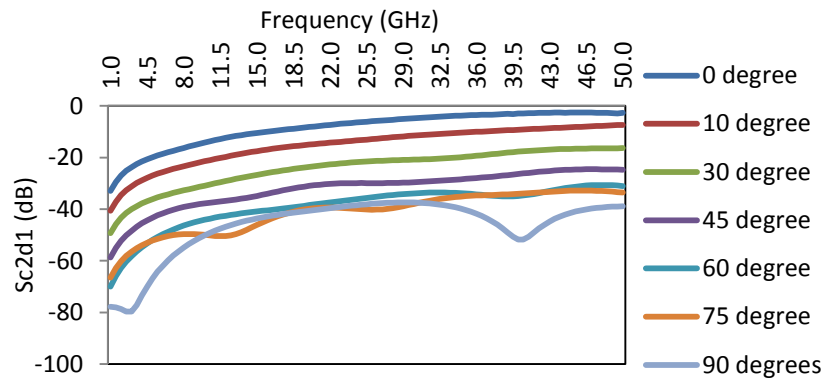
(c) Differential to common mode conversion loss.
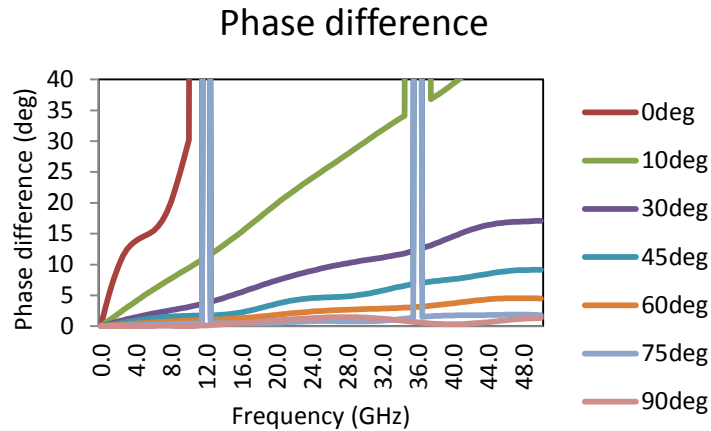
Phase difference

(d) Phase difference.

Figure 35. (a) Differential to differential return loss. (b) Differential to differential return loss (c) Differential to common mode conversion loss (d) Phase difference for 0 degree to 90 degree angle of rotation.

From Figure 35 at 90 degree angle of rotation, differential to differential insertion loss is close to -0.4dB, mode conversion loss is below -40dB and phase difference is below 5 deg.

We can see improvement in insertion loss and mode conversion loss as we rotate the transmission lines from 0 degree to 90 degree angle of rotation and phase difference is close to zero degrees at 90 degree angle of rotation. The peaks in phase difference plot refer to 350 degree phase difference.

This was the response for a basic model. Moving to complex structures, a loosely woven spread weave (1078) is considered and simulations were performed to analyze fiber weave effects on differential pair.

4.2 1078 Spread weave

Specifications for the 1078 Spread weave obtained from the manufacturers are

- 53X53 bundles/sq inch

- Cloth thickness: 28µm.

- Total number of fibers:100 fibers/bundle

- Diameter of the fiber: 5µm.

After calculations

- Pitch: 15.4 mils.

- Diameter: 2.28mils.

Using these specifications I have designed 1078 spread weave with the same dimensions as shown in Figure 36.
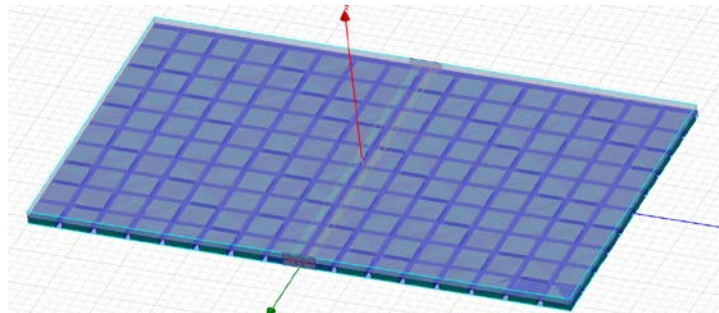
Figure 36. 1078 Spread weave with 0.25in transmission lines.

Transmission lines on the anisotropic substrate are rotated from zero degree to 45 degrees (Since the structure is symmetrical, 45 degree to 90 degree rotation will be same as 45 degree to zero degree rotation) and phase angle plots for each angle of rotation is shown in Figure 37.

(a) Zero degree

(b) 10 degree

(c) 20 degree

49
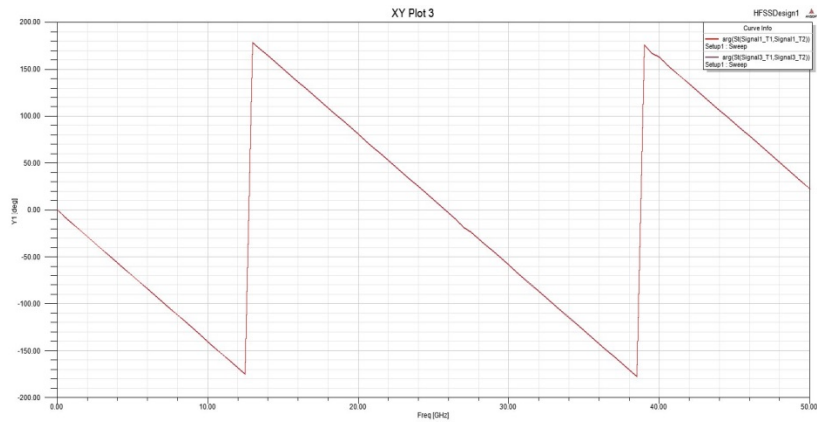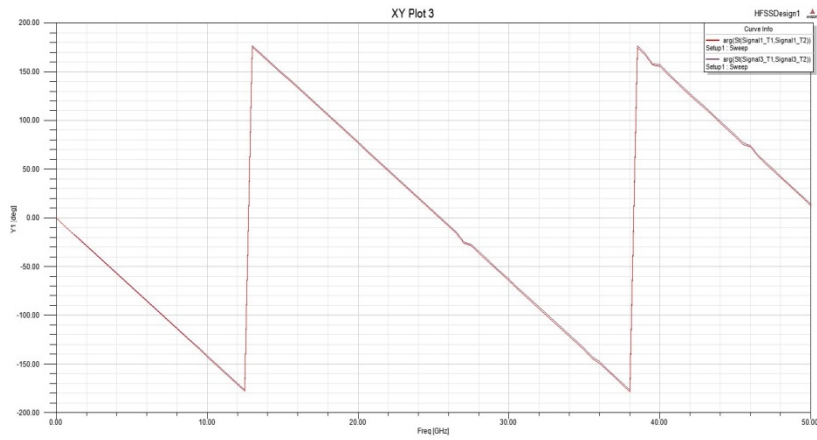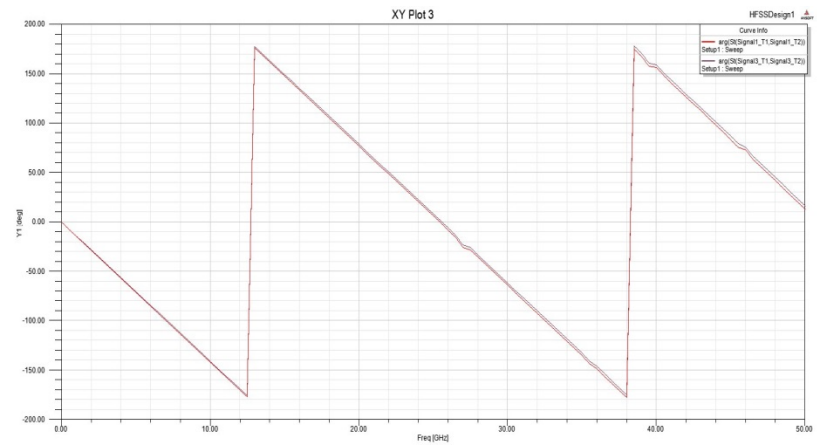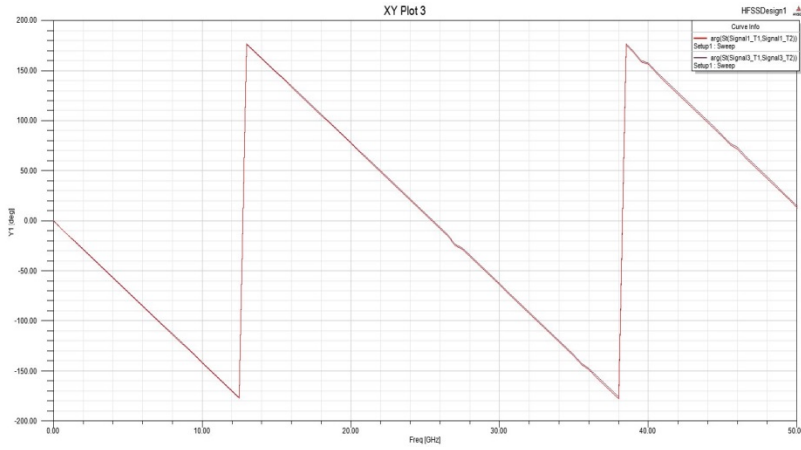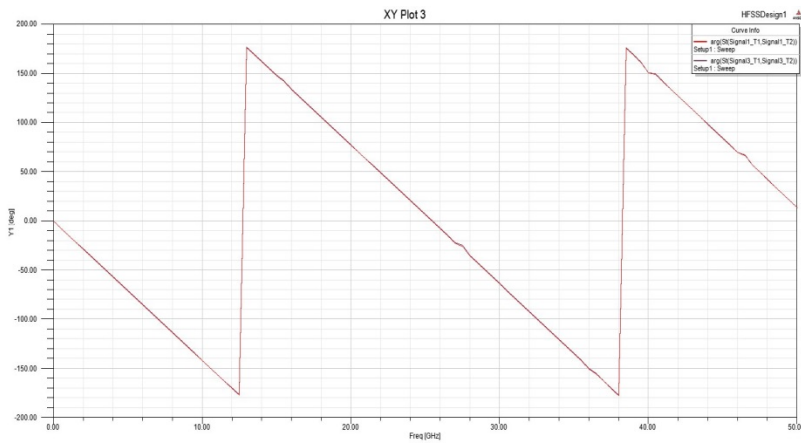
(d) 30 degree

(e) 45 degree
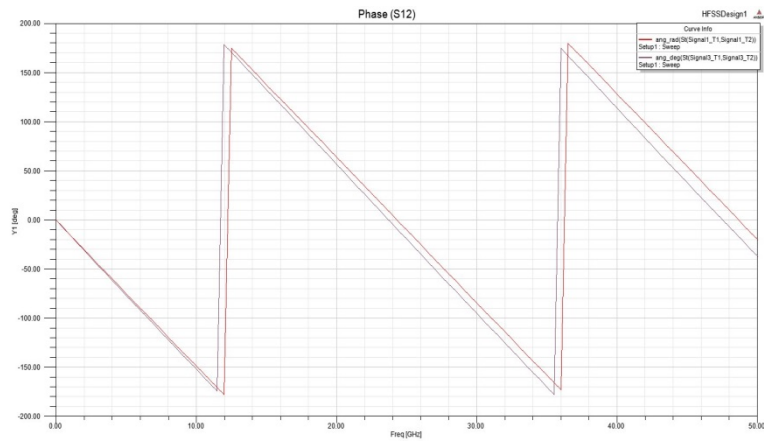
Figure 37. Phase angle plots for (a) Zero degree (b) 10 degree (c) 20 degree (d) 30 degree (e) 45

degree angle of rotation.

Phase difference (delta) at each angle of rotation is shown in Figure 38.
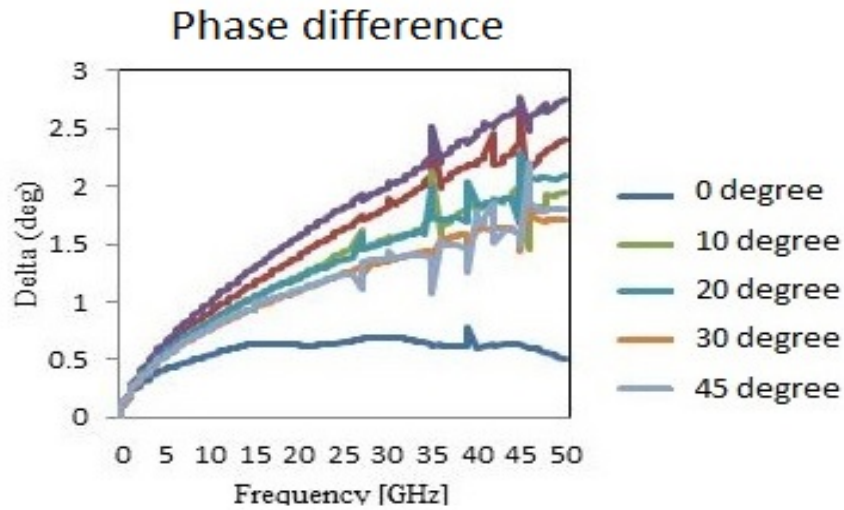
Figure 38. Phase difference for 0 degree to 45 degree angle of rotation

Terminal S-parameters are extracted from HFSS and inserted into a 4-port network model in ADS shown in Figure 39.
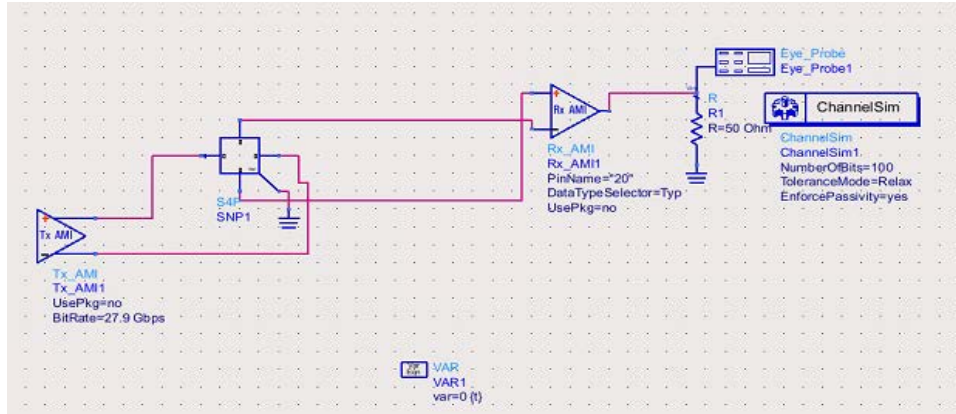
Figure 39. 4-port network ADS model.

Simulations are performed at 28gbps bit rate and BER contours ($1X10^{-13}$) are examined at the receiver. Equalization techniques are applied at the receiver to improve the area of BER contour. Values for height, width and area of the BER contour for 0.25in transmission lines are given in Table 1 and a graph is plotted shown in Figure 40.

Angle of rotation	Height (V)	Width (ps)	Area (V-ps)
0	0.414	12.90	5.39332
10	0.450	11.29	5.39328
20	0.418	13.44	5.91354
30	0.422	13.62	5.78772
45	0.436	11.65	5.13422

Table 1. Height, width and Area for 1078 spread weave.
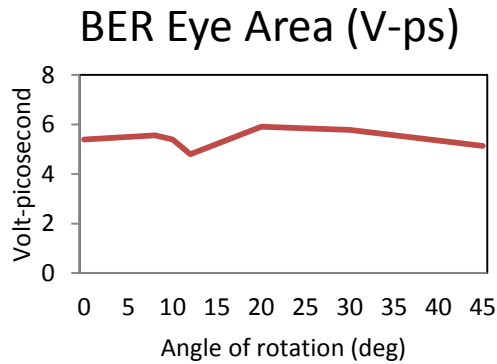
Figure 40. BER contour Area (1×10^{-13}) vs. angle of rotation

Values given in the Table 1 are optimized values in terms of height, width and area of the BER contours. BER Area plot does not provide any information about maximum area with respect to angle of rotation. The reason being, the length of the transmission lines is too small to account fiber weave effects. So the length of the transmission lines is increased.

The length of the transmission lines are increased to 0.5in to account the effects of fiber weave shown in Figure 41.
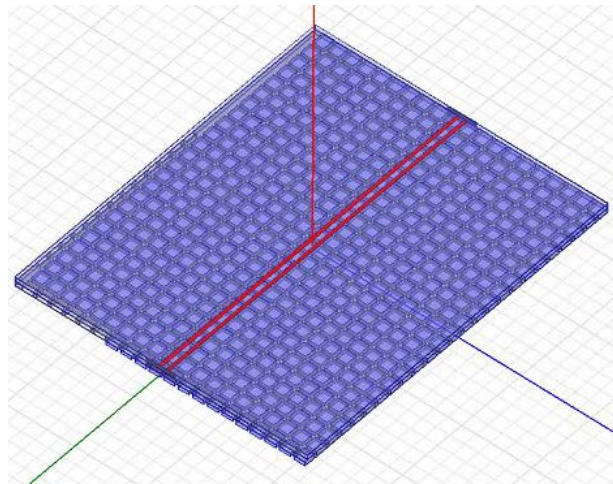
Figure 41. 1078 with spread weave with 0.5in transmission lines.

The source for differential skew in anisotropic substrate also depends on position of transmission lines. This can be explained from Figure 42. In Figure 42(a) we can see that differential pair is mounted on the outer   edges   of   the

(a)

(b)

(c)

Figure 42. (a) Position 1 (b) Position 2 (c) Position 3

fiber. In Figure 42(b) one of the differential pair is mounted on the fiber and other is mounted on combination of resin and fiber and in Figure 42(c) differential pair is mounted between the two fibers. Position 1 and position 2 introduce differential skew but position 3 introduces negligible skew (Figure 45) since medium under the differential pair is homogenous.

Simulations are performed for three positions and phase angle plots for 0 degree to 45 degree angle of rotation are plotted.

Phase angle plots for position 1 are shown in Figure 43.
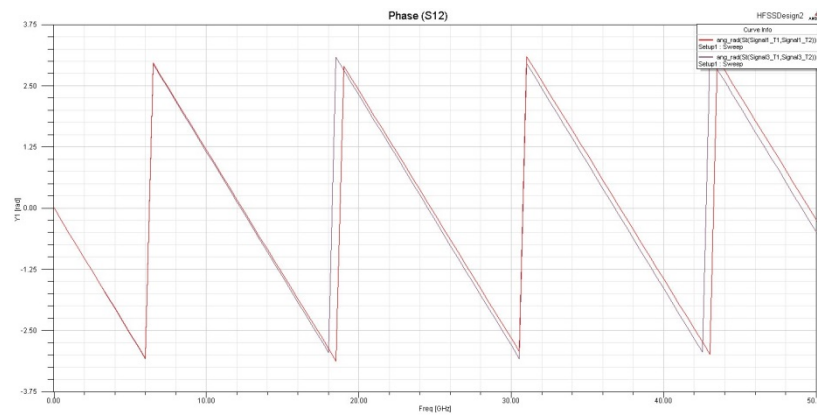
(a) Zero degree
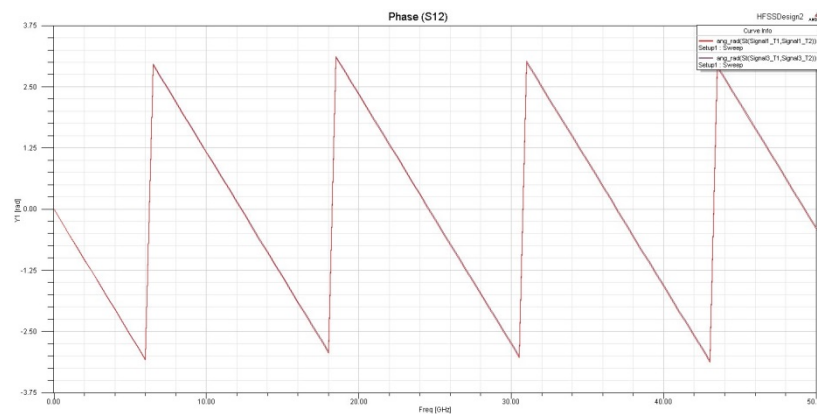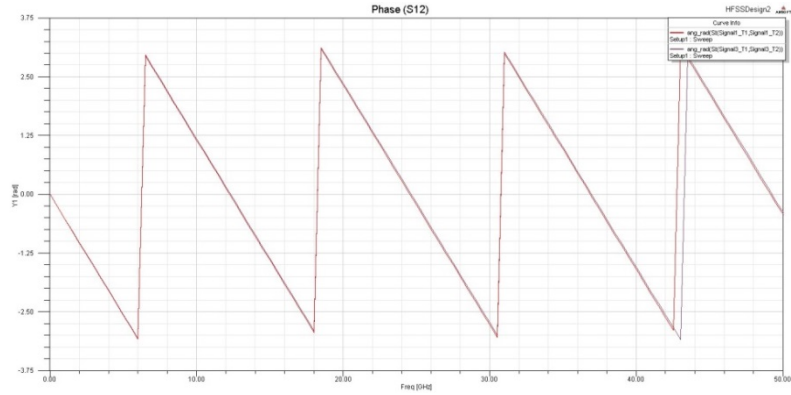
(b) 10 degree
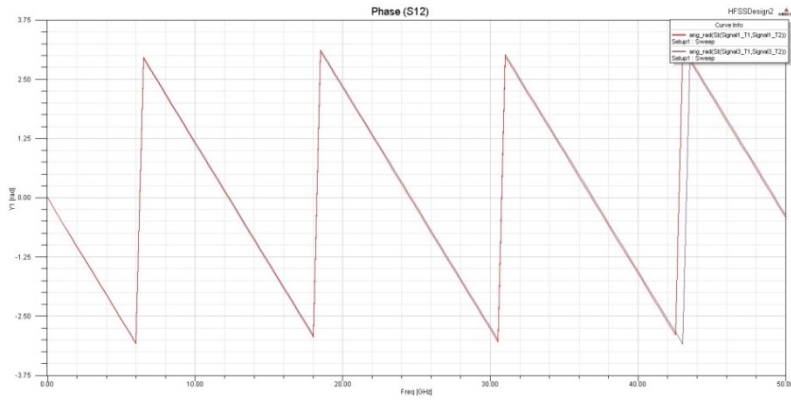
(c) 20 degree
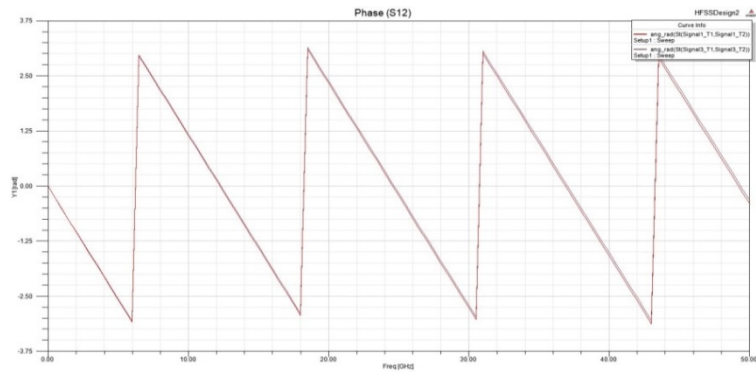
(d) 30 degree

(e) 45 degree

Figure 43. (a) zero degree (b) 10 degree (c) 20 degree (d) 30 degree (e) 45 degree angle of

rotation for position 1.

Phase angle plots for position 2 are shown in Figure 44.
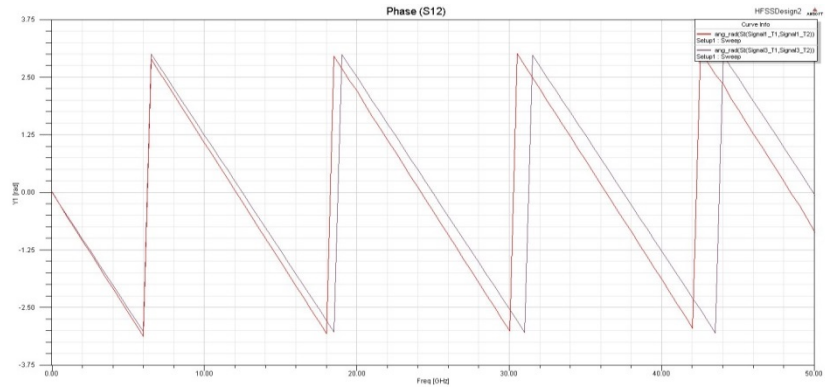
(a) zero degree
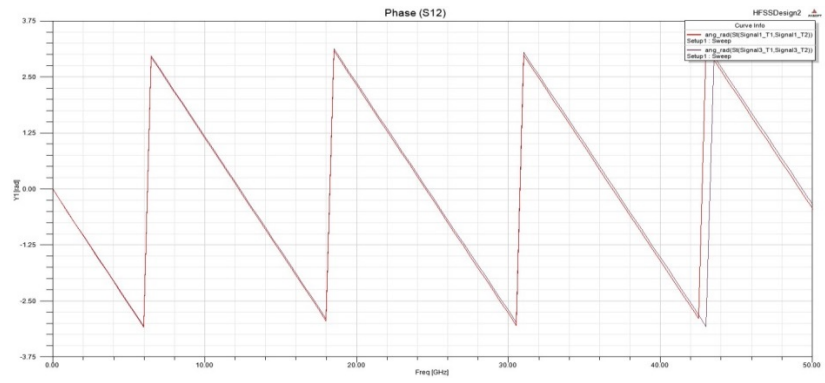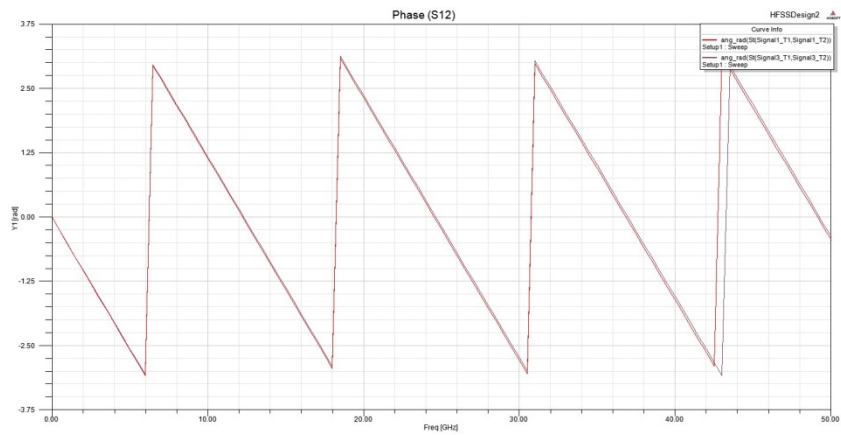
(b) 10 degree
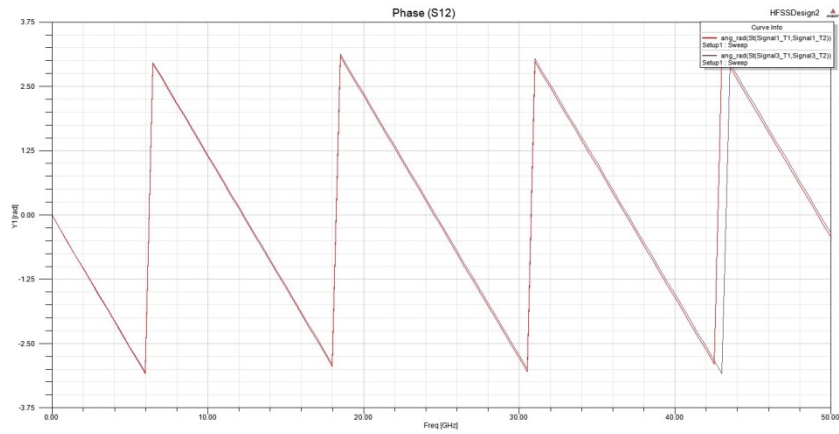
(c) 20 degree
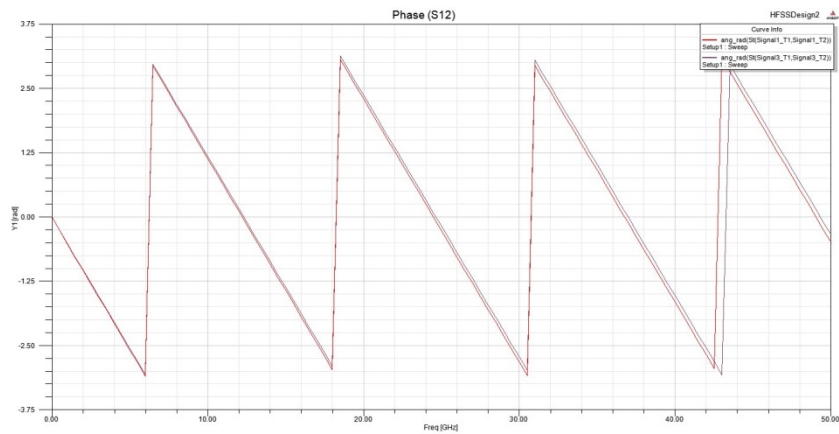
(d) 30 degree

(e) 45 degree

Figure 44. (a) Zero degree (b) 10 degree (c) 20 degree (d) 30 degree

(e) 45 degree angle of rotation for position 2

Phase angle plots for position 3 are shown in Figure 45.
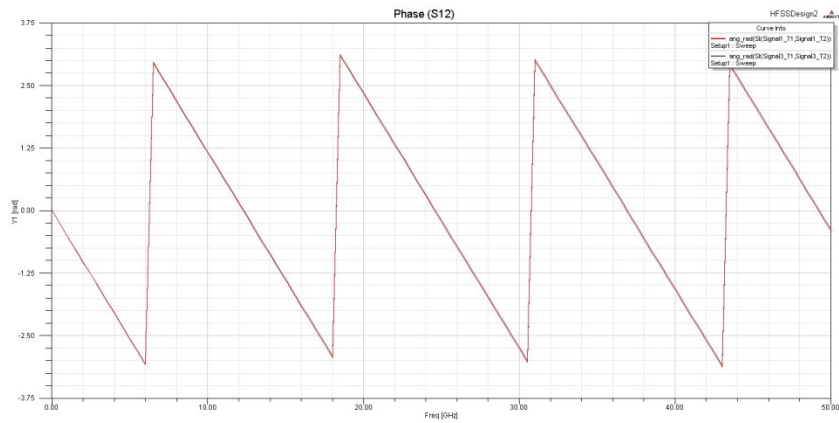
(a) Zero degree
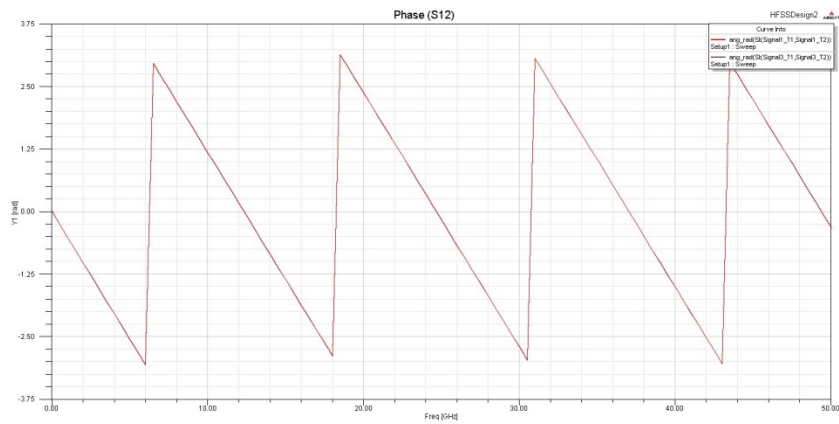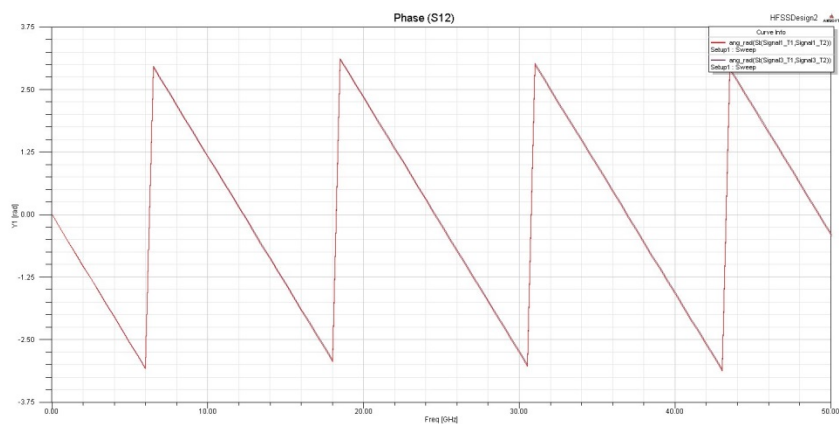
(b) 10 degree
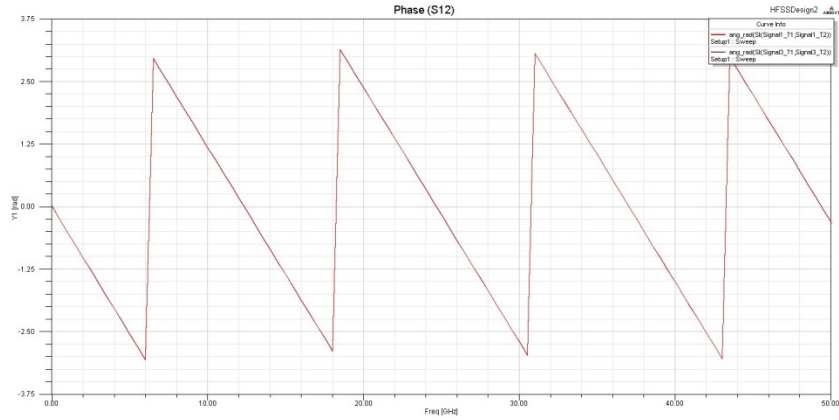
(c) 20 degree
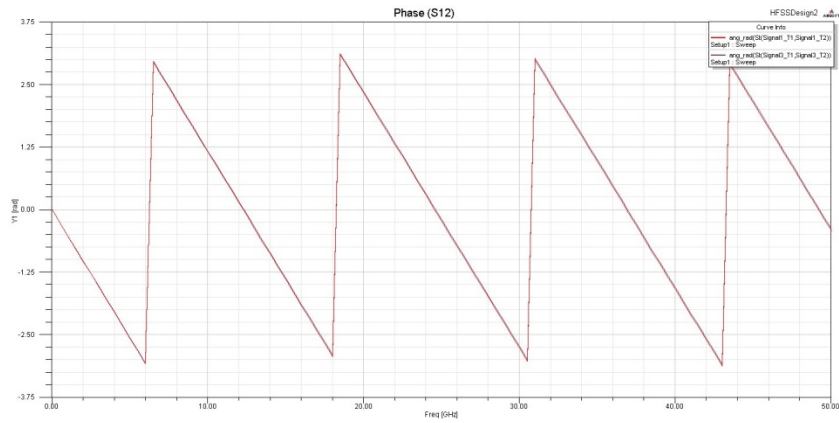
(d) 30 degree

(e) 45 degree

Figure 45. (a) Zero degree (b) 10 degree (c) 20 degree (d) 30 degree

(e) 45 degree angle of rotation for position 3.

Differential to differential return loss (S_{d1d1}), differential to differential insertion loss (S_{d2d1}), differential to common mode conversion loss (S_{c2d1}) and phase difference plots are shown in Figure 46 for position 1.

Differential to differential return loss
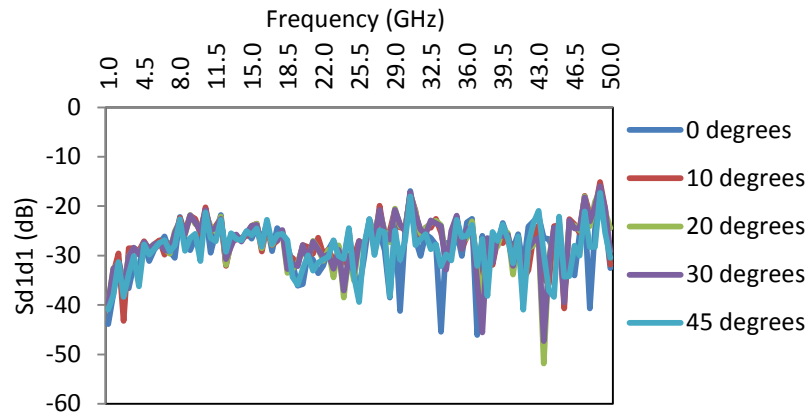
(a) Differential to differential return loss.

Differential to differential insertion loss
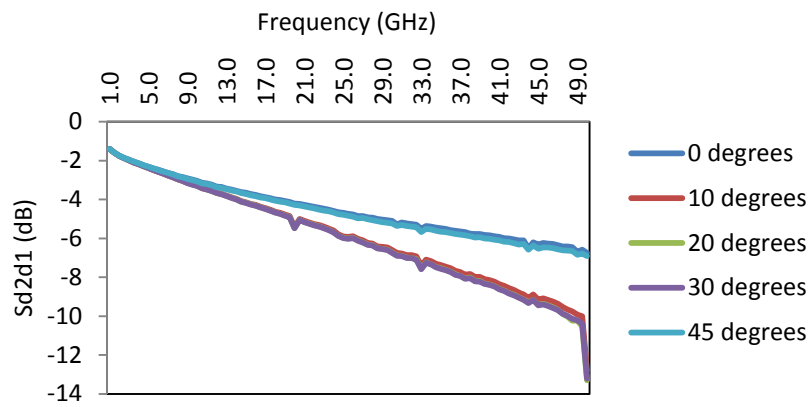
(b) Differential to differential insertion loss.

Differential to common mode conversion loss
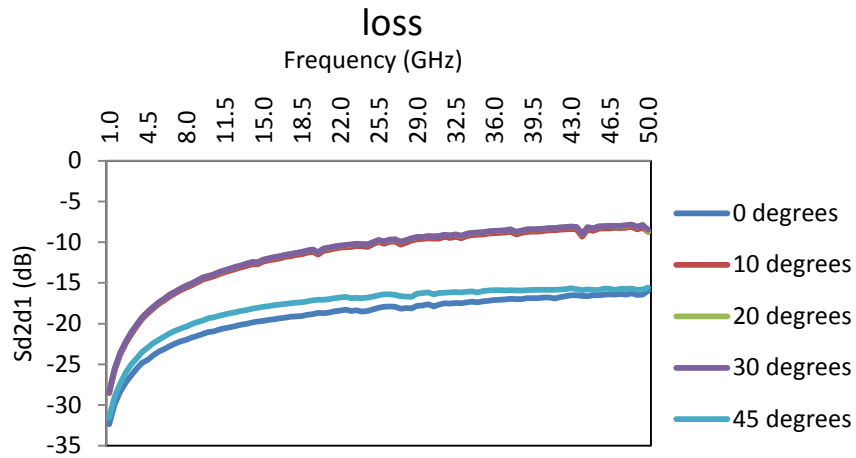
(c) Differential to common mode conversion loss.
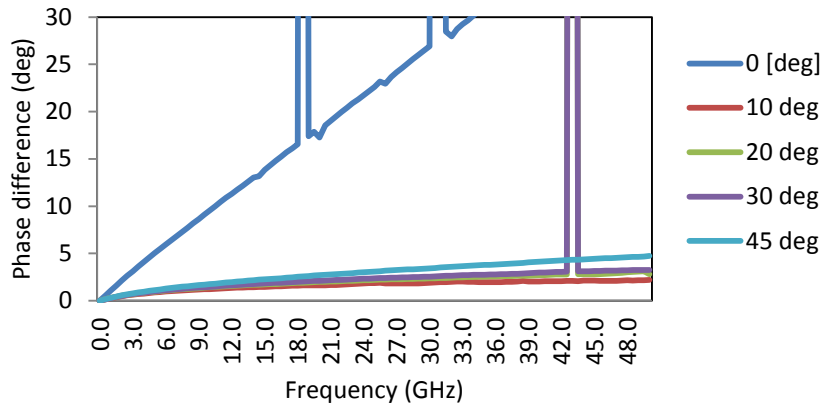
Phase difference

(d) Phase difference for 0.5in.

Figure 46. (a) Differential to differential return loss (b) Differential to differential insertion loss (c) Differential to common mode conversion loss (d) Phase difference for position 1.

Differential to differential return loss (S_{d1d1}), differential to differential insertion loss (S_{d2d1}), differential to common mode conversion loss (S_{c2d1}) and phase difference plots are shown in Figure 47 for position 2.

Differential to differential return loss
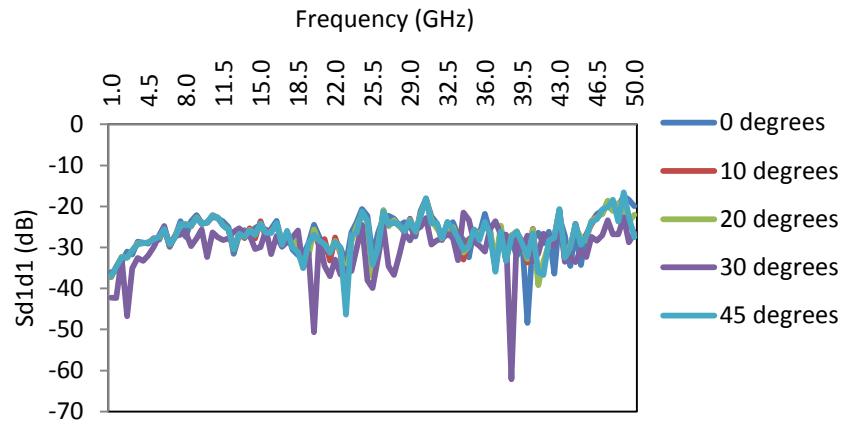
Frequency (GHz)

(a) Differential to differential return loss.

Differential to differential insertion loss

Frequency (GHz)

(b) Differential to differential insertion loss.

Differential to common mode conversion

Frequency (GHz)
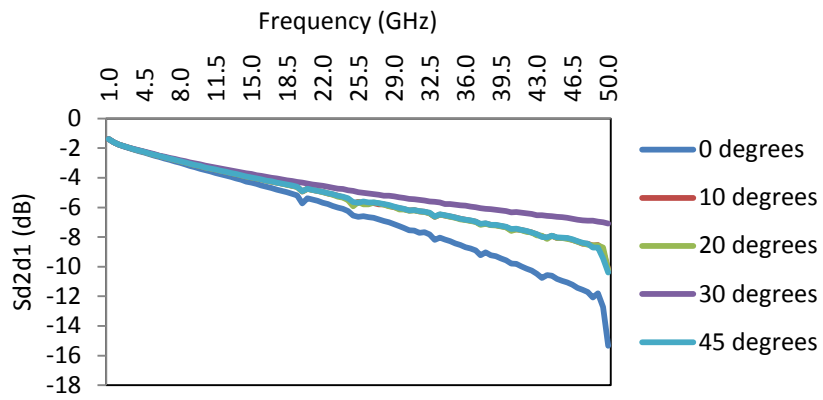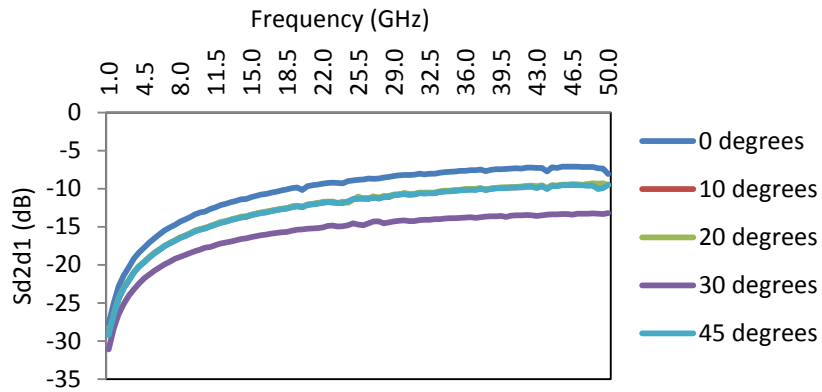
(c) Differential to common mode conversion loss.
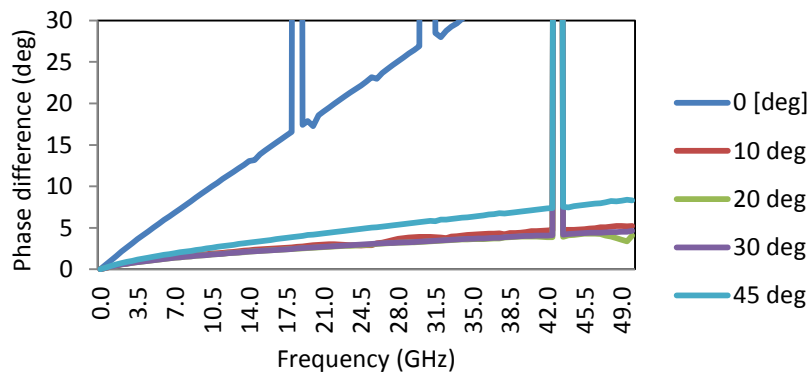
Phase difference

(d) Phase difference for 0.5in.

Figure 47. (a) Differential to differential return loss (b) Differential to differential insertion loss

(c) Differential to common mode conversion loss (d) Phase difference for position 2.

Differential to differential return loss (S_{d1d1}), differential to differential insertion loss (S_{d2d1}), differential to common mode conversion loss (S_{c2d1}) and phase difference plots are shown in Figure 48 for position 3.

Differential to differential return loss
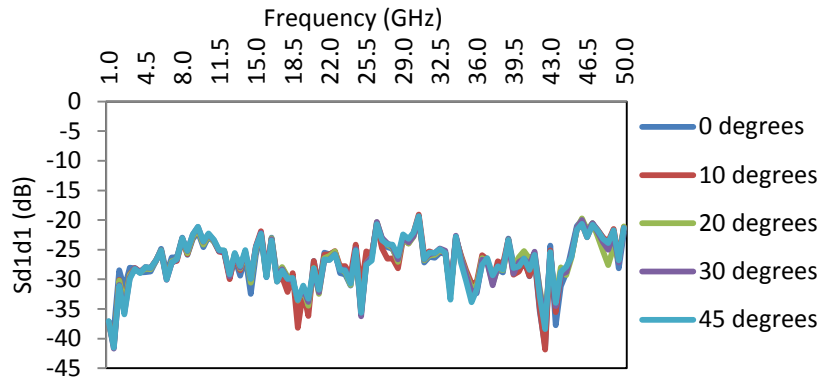
(a) Differential to differential return loss.

Differential to differential insertion loss

(b) Differential to differential insertion loss.

64
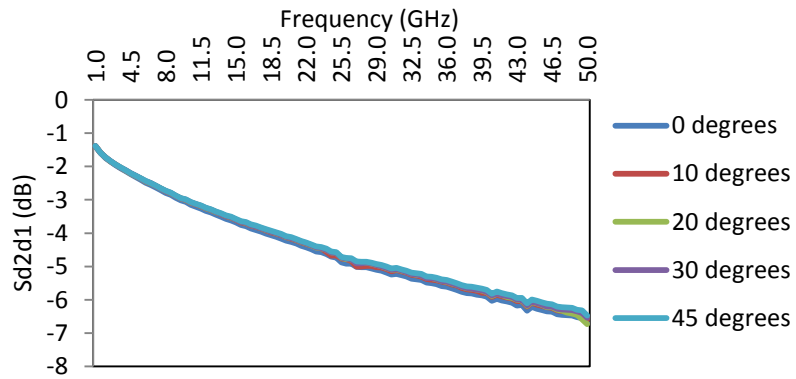
Differential to common mode conversion
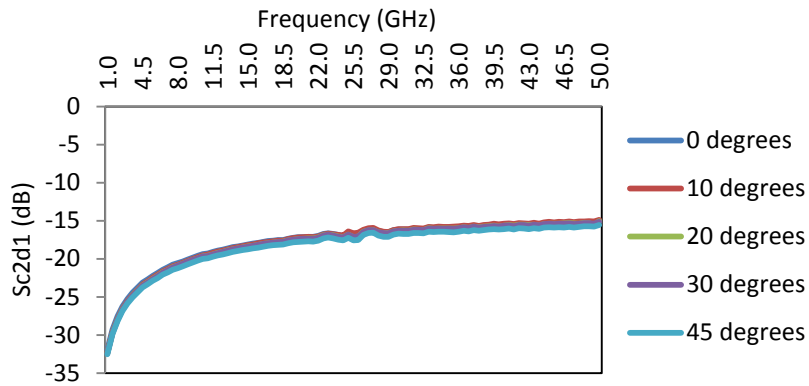
(c) Differential to common mode conversion loss.
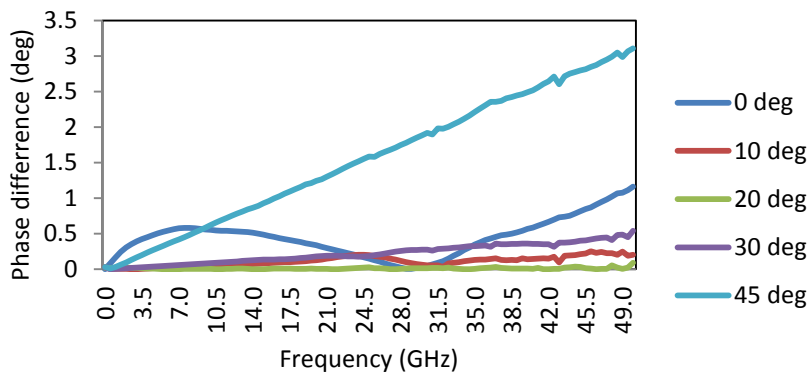
Phase difference

(d) Phase difference for 0.5in.

Figure 48. (a) Differential to differential return loss (b) Differential to differential insertion loss

(c) Differential to common mode conversion loss (d) Phase difference plots for position 3.

S-parameters are extrapolated to larger lengths as shown in Figure 49. Signal integrity analyses are performed in terms of height, width and area of the BER contours. Equalization techniques are applied at the receiver to optimize the signal.
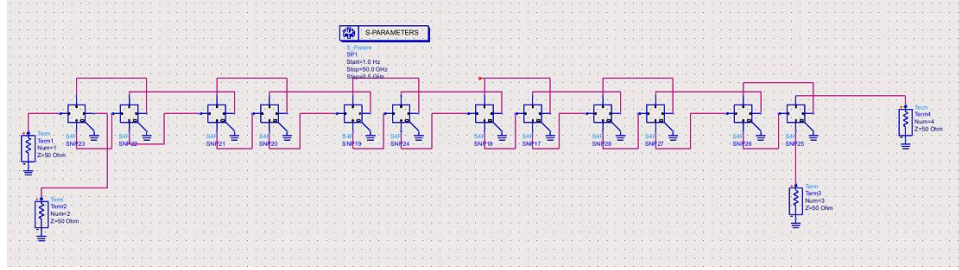
Figure 49. Increasing the length of the transmission lines to 6in

Values for height, width and area of BER contours for three positions are given in Table 2.

degree	Without optimization			With optimization		
	Height (V)	Width (ps)	Area (V-ps)	Height (V)	Width (ps)	Area (V-ps)
0	0.186	14.7	2.7342	0.37	12.62	5.0394
10	0.153	9.319	1.425	0.38	12.72	4.836
20	0.206	13.98	2.8798	0.38	12.37	4.7006
30	0.202	13.44	2.7148	0.379	12.37	4.68823
45	0.109	9	0.952	0.37	16.13	5.9681

(a) Position 1

degree	Without optimization			With optimization		
	Height (V)	Width (ps)	Area (V-ps)	Height (V)	Width (ps)	Area (V-ps)
0	0.172	12.01	2.064	0.383	13.8	5.286
10	0.16	11.89	1.895	0.364	12.01	4.372
20	0.148	10.39	1.539	0.347	12.01	4.161
30	0.152	13.37	1.885	0.4	15.95	6.328
45	0.188	13	2.46	0.375	15.23	5.713

(b) Position 2

degree	Without optimization			With optimization		
	Height (V)	Width (ps)	Area (V-ps)	Height (V)	Width (ps)	Area (V-ps)
0	0.171	15.77	2.696	0.377	15.95	6.016
10	0.178	9.677	1.721	0.362	15.59	5.572
20	0.136	10.39	1.421	0.355	11.65	4.138
30	0.142	10.57	1.497	0.342	11.47	3.923
45	0.143	10.22	1.457	0.336	11.83	3.976

(c) Position 3

Table 2. BER contour values for (a) Position 1 (b) Position 2 (c) Position 3

A graph is plotted for the values given in Table 2 are shown in Figure 50.

BER Eye Area vs Angle of rotation
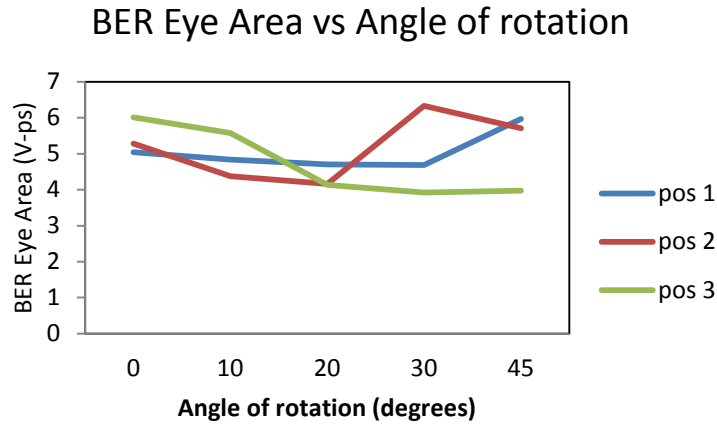
Figure 50. Graph for BER contour area for three positions.

For position 1

From Figure 46(a) differential to differential return loss is below -20dB, differential to differential insertion loss is close to -6dB and differential to common mode conversion loss is low (<-15dB) for 45 degree angle of rotation, from phase difference plot shown in Figure 46(d) there occurs a phase difference close to zero (<5 degrees). Signal integrity analysis is performed and equalization techniques are applied to find maximum area of BER contour at 45 degree angle of rotation. Peaks in the phase difference plots represent a phase difference of 350 degrees between differential pair.

For position 2

From Figure 47(a) differential to differential return loss is below -20dB, differential to differential insertion loss is close to -6dB and differential to common mode conversion loss is low (<-15dB) for 30 degree angle of rotation, from phase difference plot shown in Figure 47(d) a phase difference of 350 degrees at 43GHz from 10 degree to 45 degree angle of rotation. Signal integrity analysis is performed and equalization techniques are applied to find maximum area of BER contour at 35 degree angle of rotation.

For position 3

From Figure 48(a) differential to differential return loss is below -20dB, differential to differential insertion loss is close to -6dB, differential to common mode conversion loss is low (<-15dB) and phase difference is close to zero (< 5 degrees) for zero degrees to 45 degrees angle of rotation. Signal integrity analysis is performed and equalization techniques are applied to find maximum optimization at zero degrees and as we rotate area decreases to 80% of the maximum value.

4.2.1 Length factor

Length of the transmission lines also plays an important role in signal integrity. Maximum length of the differential pair is found out with respect to three positions for all angles of rotation.

Values of Height, width and area of BER contour with respect to length of transmission lines for position 1 with and without optimization is given in Table 3.

0 degree

Length (in)	Without optimization			With optimization		
	Height (V)	Width (ps)	Area (V-ps)	Height (V)	Width (ps)	Area (V-ps)
1	0.244	20.43	4.985	0.244	20.43	4.985
2	0.331	19.18	6.353	0.331	19.18	6.353
3	0.324	17.03	5.515	0.324	17.03	5.515
4	0.34	16.13	5.542	0.379	14.87	5.643
5	0.278	12.9	3.583	0.374	15.05	5.624
6	0.184	12.9	2.378	0.37	13.62	5.093
7	0.076	11.29	0.85804	0.221	6.452	1.42589
8	0.081	5.018	0.4064	0.158	6.093	0.962
9	0	0	0	0.108	6.093	0.6578
10	0	0	0	0.063	3.58	0.2249
11	0	0	0	0	0	0

(a) 0 degree

10 degree

Length (in)	Without optimization			With optimization		
	Height (V)	Width (ps)	Area (V-ps)	Height (V)	Width (ps)	Area (V-ps)
1	0.234	20.25	4.731	0.413	12.01	4.963
2	0.284	17.74	5.047	0.284	17.74	5.047
3	0.32	17.92	5.73	0.32	17.92	5.73
4	0.33	17.2	5.674	0.33	17.2	5.674
5	0.275	13.08	3.62	0.364	11.29	4.105
6	0.158	9.498	1.499	0.38	12.72	4.8336
7	0.079	0.914	0.723	0.208	6.989	1.4537
8	0.055	7.527	0.414	0.164	5.194	0.9684
9	0	0	0	0.111	6.093	0.6785
10	0	0	0	0.061	3.405	0.21
11	0	0	0	0	0	0

(b) 10 degree

20 degree

Length (in)	Without optimization			With optimization		
	Height (V)	Width (ps)	Area (V-ps)	Height (V)	Width (ps)	Area (V-ps)
1	0.233	20.43	4.757	0.417	12.01	5
2	0.283	18.46	5.23	0.283	18.46	5.23
3	0.312	17.2	5.375	0.312	17.2	5.375
4	0.33	17.2	5.674	0.412	14.16	5.835
5	0.287	13.08	3.684	0.378	14.7	5.549
6	0.206	13.98	2.8798	0.38	12.37	4.7006
7	0.077	1.11	0.08547	0.221	6.81	1.505
8	0.049	8.065	0.395185	0.162	6.093	0.957
9	0	0	0	0.109	6.093	0.66
10	0	0	0	0.06	3.389	0.2
11	0	0	0	0	0	0

(c) 20 degree

30 degree

Length (in)	Without optimization			With optimization		
	Height (V)	Width (ps)	Area (V-ps)	Height (V)	Width (ps)	Area (V-ps)
1	0.234	20	4.77	0.426	11.83	5.033
2	0.301	19.2	5.781	0.301	19.2	5.781

3	0.319	16.67	5.324	0.319	16.67	5.324
4	0.33	17	5.626	0.33	17	5.626
5	0.291	12.9	3.752	0.39	14.87	5.807
6	0.202	13.44	2.748	0.379	12.37	4.688
7	0.082	12.19	0.099	0.218	6.81	1.484
8	0.015	3.047	0.395185	0.194	5.197	1
9	0	0	0	0.108	6.093	0.66
10	0	0	0	0.064	3.226	0.206
11	0	0	0	0	0	0

(d) 30 degree

45 degree

	Without optimization			With optimization		
Length (in)	Height (V)	Width (ps)	Area (V-ps)	Height (V)	Width (ps)	Area (V-ps)
1	0.249	20.4	5.084	0.249	20.4	5.084
2	0.315	20	6.32	0.315	20	6.32
3	0.319	18.64	5.967	0.319	18.64	5.967
4	0.343	18.78	6.277	0.343	18.78	6.277
5	0.272	13.62	3.711	0.376	15.59	5.869
6	0.109	8.781	0.9549	0.37	16.13	5.9681
7	0.092	14.34	0.131928	0.233	6.81	1.58673
8	0.047	7.706	0.362	0.164	6.452	1.1
9	0	0	0	0.105	5.914	0.62
10	0	0	0	0.049	2.688	0.132
11	0	0	0	0	0	0

(e) 45 degree

Table 3. BER contour values for (a) 0 degree (b) 10 degree (c) 20 degree (d) 30 degree (e) 45

degree

Values of Height, width and area of BER contour with respect to length of transmission

lines for position 2 with and without optimization is given in   Table 4.

0 degree

	Without optimization			With optimization		
Length (in)	Height (V)	Width (ps)	Area (V-ps)	Height (V)	Width (ps)	Area (V-ps)
1	0.249	20.25	5.045	0.249	20.25	5.045
2	0.298	19.53	5.82	0.298	19.53	5.82

3	0.319	18.64	5.947	0.319	18.64	5.947
4	0.331	18.1	6	0.331	18.1	6
5	0.257	14.87	3.816	0.371	10.93	4.054
6	0.172	12.01	2.064	0.383	13.8	5.286
7	0.082	10.22	0.8241	0.221	6.093	1.349
8	0.1	1.61	0.0135	0.112	5.376	0.6
9	0	0	0	0.101	4.839	0.4769
10	0	0	0	0.029	1.434	0.0415
11	0	0	0	0	0	0

(a) 0 degree

10 degree

	Without optimization			With optimization		
Length	Height (V)	Width (ps)	Area (V-ps)	Height (V)	Width (ps)	Area (V-ps)
1	0.212	19.35	4.15	0.422	12.19	5.139
2	0.287	18.28	5.254	0.287	18.28	5.254
3	0.307	17.03	5.224	0.307	17.03	5.224
4	0.33	19.89	6.562	0.33	19.89	6.562
5	0.287	13.98	4.014	0.37	11.47	4.243
6	0.16	11.83	1.8985	0.364	12.01	4.372
7	0.081	1.044	0.8091	0.196	6.631	1.3
8	0.005	1.434	0.0072	0.127	6.093	0.7746
9	0	0	0	0.109	6.093	0.6628
10	0	0	0	0.049	2.688	0.1323
11	0	0	0	0	0	0

(b) 10 degree

20 degree

	Without optimization			With optimization		
Length	Height (V)	Width (ps)	Area (V-ps)	Height (V)	Width (ps)	Area (V-ps)
1	0.213	20.25	4.316	0.416	11.29	4.695
2	0.278	18.46	5.128	0.278	18.46	5.128
3	0.301	17.2	5.174	0.301	17.2	5.174
4	0.326	17.56	5.73	0.326	17.56	5.73
5	0.285	13.08	3.731	0.373	10.93	4.074
6	0.148	10.39	1.539	0.347	12.01	4.161
7	0.048	9.498	0.4536	0.183	6.81	1.244
8	0.005	1.264	0.006424	0.123	6.272	0.7736

9	0	0	0	0.105	6.093	0.6427
10	0	0	0	0.054	2.509	0.1344
11	0	0	0	0	0	0

(c) 20 degree

30 degree

	Without optimization				With optimization	
Length	Height (V)	Width (ps)	Area (V-ps)	Height (V)	Width (ps)	Area (V-ps)
1	0.209	19.89	4.156	0.418	11.65	4.866
2	0.292	20.61	6	0.292	20.61	6
3	0.333	17.56	5.855	0.333	17.56	5.855
4	0.334	18.28	6.102	0.334	18.28	6.102
5	0.278	13.08	3.639	0.366	11.11	4.066
6	0.177	16.85	2.988	0.4	15.95	6.328
7	0.071	10.04	0.7099	0.23	6.093	1.401
8	0.001	1.792	0.00022	0.128	6.272	0.8045
9	0	0	0	0.106	6.093	0.65
10	0	0	0	0.063	3.226	0.2022
11	0	0	0	0	0	0

(d) 30 degree

45 degree

	Without optimization			With optimization		
Length	Height (V)	Width (ps)	Area (V-ps)	Height (V)	Width (ps)	Area (V-ps)
1	0.231	20.43	4.72	0.418	1.2	5
2	0.296	19.35	5.72	0.296	19.35	5.72
3	0.332	17.38	5.779	0.332	17.38	5.779
4	0.33	18.1	5.974	0.33	18.1	5.974
5	0.272	13.26	3.611	0.365	10.93	3.99
6	0.188	13.08	2.406	0.375	15.23	5.713
7	0.071	10.04	0.7099	0.2	6.631	1.327
8	0.004	0.891	0.00346	0.125	6.272	0.7829
9	0	0	0	0.107	5.914	0.6302
10	0	0	0	0.059	3.226	0.1899
11	0	0	0	0	0	0

(e) 45 degree

Table 4. BER contour values for (a) 0 degree (b) 10 degree (c) 20 degree (d) 30 degree (e) 45

degree

Values of Height, width and area of BER contour with respect to length of transmission

lines for position 3 with and without optimization is given in   Table 5.

0 degree

Length	Without optimization			With optimization		
(in)	Height (V)	Width (ps)	Area (V-ps)	Height (V)	Width (ps)	Area (V-ps)
1	0.245	20.43	4.997	0.245	20.43	4.997
2	0.311	18.1	5.627	0.311	18.1	5.627
3	0.314	17.38	5.455	0.314	17.38	5.455
4	0.312	16.67	5.195	0.312	16.67	5.195
5	0.285	14.87	4.242	0.377	15.41	5.812
6	0.171	15.77	2.696	0.377	15.95	6.016
7	0.066	9.14	0.6	0.208	6.631	1.381
8	0.034	4.301	0.1446	0.187	5.556	1.04
9	0	0	0	0.133	3.584	0.475
10	0	0	0	0.059	3.405	0.2
11	0	0	0	0	0	0

(a) 0 degree

10 degree

Length	Without optimization			With optimization		
(in)	Height (V)	Width (ps)	Area (V-ps)	Height (V)	Width (ps)	Area (V-ps)
1	0.224	19.71	4.425	0.419	11.83	4.955
2	0.304	17.74	5.41	0.304	17.74	5.41
3	0.314	17.38	5.455	0.314	17.38	5.455
4	0.311	16.67	5.186	0.405	14.52	5.875
5	0.285	14.87	4.242	0.384	15.05	5.786
6	0.178	9.677	1.721	0.362	15.59	5.572
7	0.086	12.01	1.029	0.224	6.631	1.488
8	0.034	5.914	0.1986	0.195	5.56	1.083
9	0.004	0.3584	0.00133	0.11	5.018	0.5529
10	0	0	0	0.074	3.763	0.2793
11	0	0	0	0	0	0

(b) 10 degree

20 degree

	Without optimization			With optimization		
Length (in)	Height (V)	Width (ps)	Area (V-ps)	Height (V)	Width (ps)	Area (V-ps)
1	0.242	2.061	4.985	0.417	12.01	5
2	0.331	18.1	5.992	0.331	18.1	5.992
3	0.341	18.28	6.23	0.341	18.28	6.23
4	0.321	16.49	5.286	0.399	13.8	5.506
5	0.289	14.87	4.292	0.375	14.87	5.585
6	0.136	10.39	1.421	0.355	11.65	4.138
7	0.077	10.22	0.786	0.219	6.631	1.455
8	0.034	4.301	0.144	0.187	5.556	1.04
9	0	0	0	0.114	4.839	0.5523
10	0	0	0	0.031	2.151	0.069
11	0	0	0	0	0	0

(c) 20 degree

30 degree

	Without optimization			With optimization		
Length (in)	Height (V)	Width (ps)	Area (V-ps)	Height (V)	Width (ps)	Area (V-ps)
1	0.224	19.71	4.425	0.419	11.83	4.955
2	0.304	17.74	5.401	0.304	17.74	5.401
3	0.338	17.92	6.058	0.338	17.92	6.058
4	0.337	17.56	5.918	0.337	17.56	5.918
5	0.285	14.87	4.242	0.377	15.41	5.812
6	0.142	10.57	1.497	0.342	11.47	3.923
7	0.066	9.14	0.6	0.208	6.631	1.381
8	0.038	5.735	0.219	0.195	5.735	1.117
9	0	0	0	0.11	4.48	0.4918
10	0	0	0	0.032	2.151	0.0692
11	0	0	0	0	0	0

(d) 30 degrees

45 degrees

	Without optimization			With optimization		
Length (in)	Height (V)	Width (ps)	Area (V-ps)	Height (V)	Width (ps)	Area (V-ps)

1	0.223	11.29	2.513	0.419	12.37	5.2
2	0.321	18.28	5.859	0.321	18.28	5.859
3	0.347	16.67	5.778	0.347	16.67	5.778
4	0.337	17.56	5.918	0.337	17.56	5.918
5	0.285	14.87	4.242	0.377	15.41	5.812
6	0.143	10.22	1.457	0.336	11.83	3.976
7	0.066	9.14	0.6	0.208	6.631	1.381
8	0.034	4.301	0.1446	0.187	5.556	1.04
9	0	0	0	0.159	3.763	0.5969
10	0	0	0	0.032	2.151	0.06
11	0	0	0	0	0	0

(e) 45 degrees

Table 5. BER contour values for (a) 0 degree (b) 10 degree (c) 20 degree (d) 30 degree (e) 45

degree

BER contour area graphs are plotted with respect to length of the transmission lines shown in

Figure 51
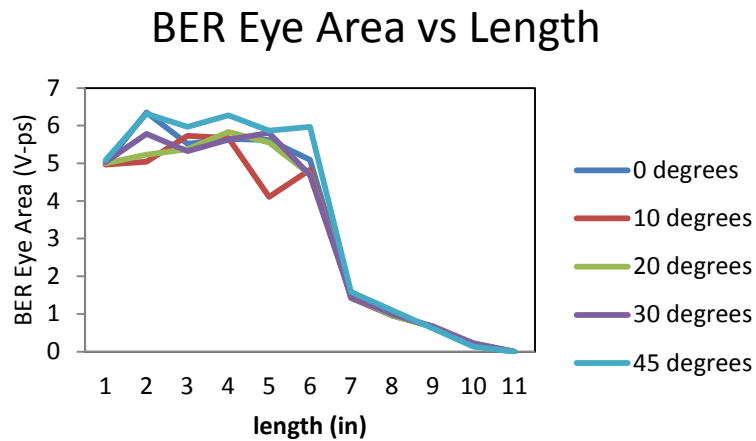
(a) Position 1

BER Eye Area vs Length
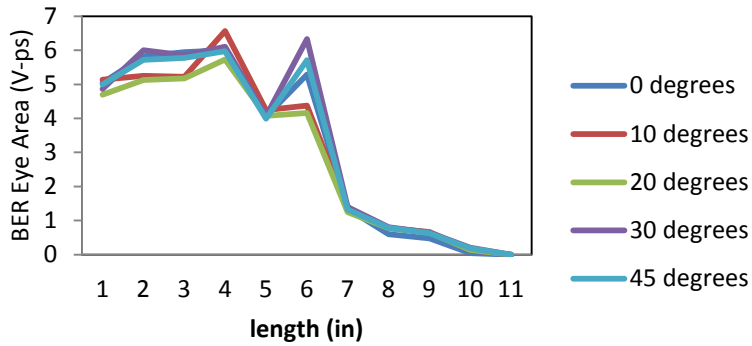
(b) Position 2

BER Eye Area vs Length
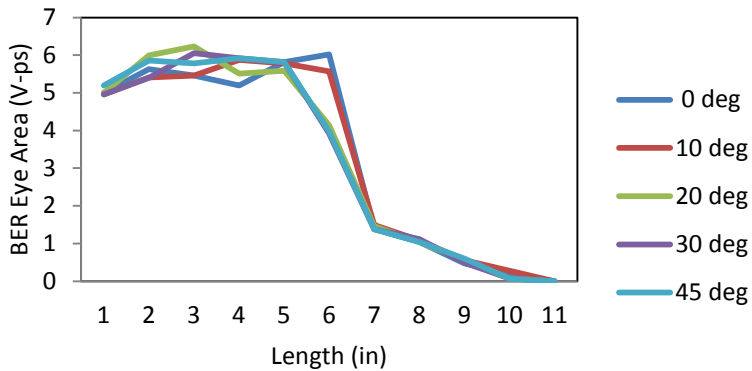
(c) Position 3

Figure 51. BER contour Area vs. length for (a) Position 1 (b) Position 2 (c) Position 3

For complex structures shown in Figure 21 often transmission lines are routed at different angles to avoid the anisotropic effect. In such cases transmission lines are extended up to a length where the BER Area curve remains constant or 80% of the maximum Area. Looking at Figure 51 we can tell that for all positions, differential pair is extended up to 6in beyond 6in BER Area would drop off to 20% of the maximum value. If we consider 20% of the maximum value as the lower cut off for BER contour area then transmission lines can extend up to 7in.

4.2.2 Insertion loss and Input impedance

Insertion loss for three positions is shown in Figure 52.
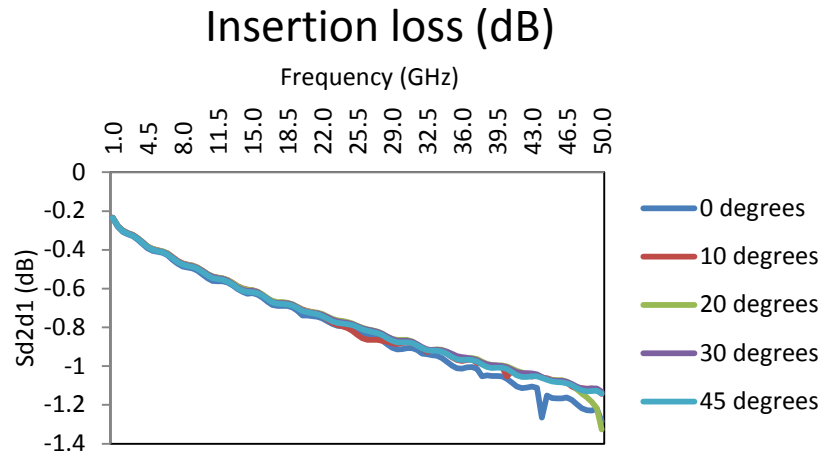
(a) Position 1
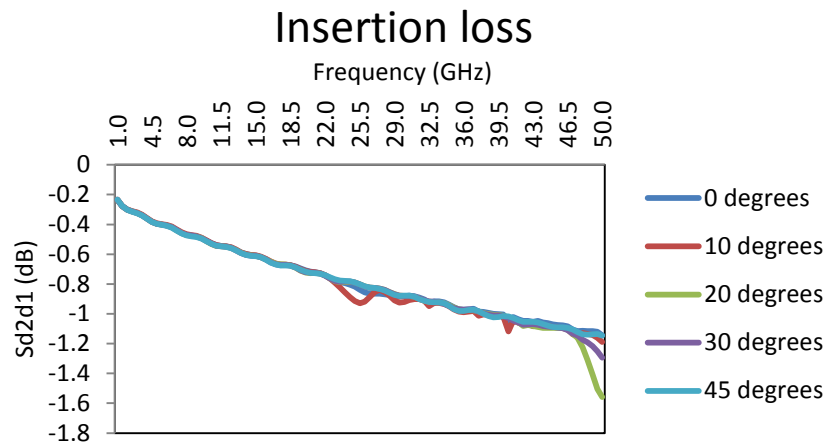
(b) Position 2
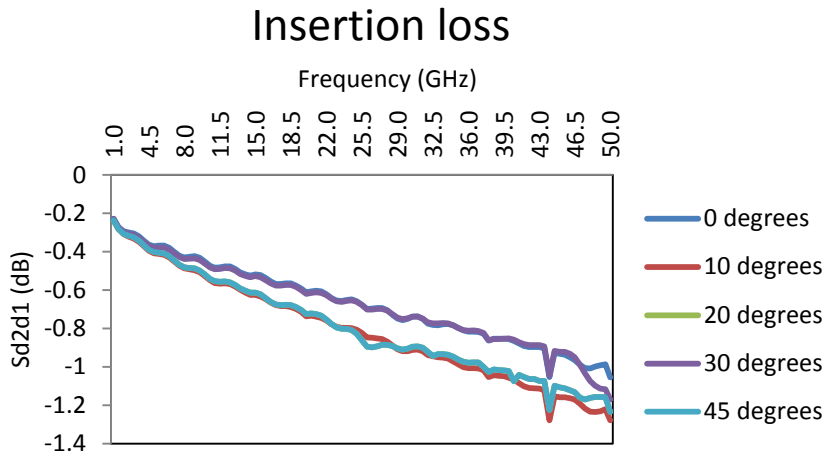
Insertion loss

(c) Position 3

Figure 52. Insertion loss for (a) Position 1 (b) Position 2 (c) Position 3

Input impedance for three positions is shown in Figure 53.

Input impedance

(a) Position 1

Input impedance
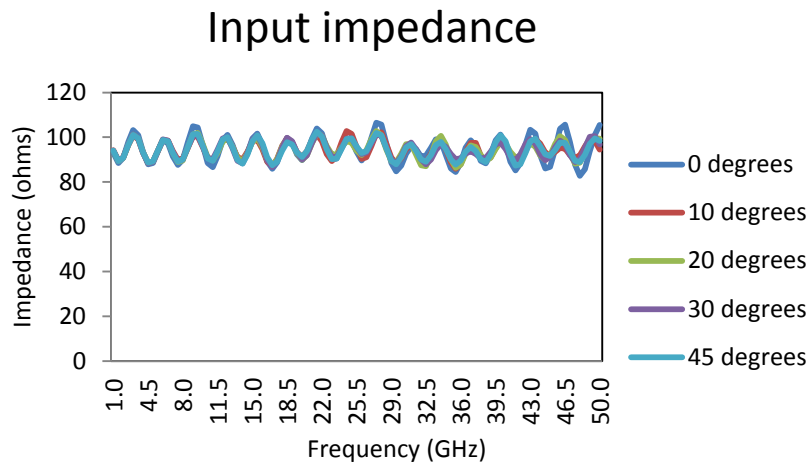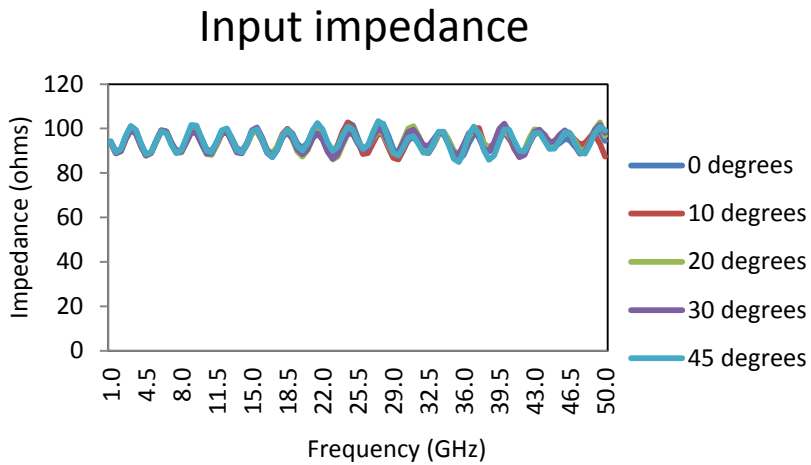
(b) Position 2
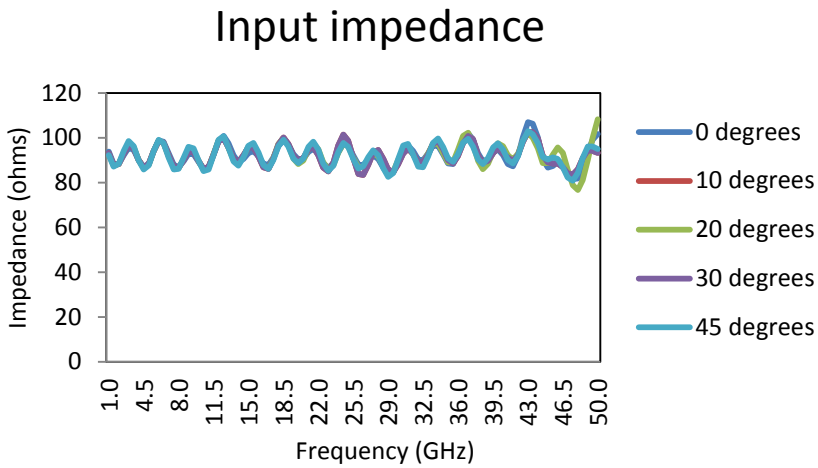
Input impedance

(c) Position 3

Figure 53. Input impedance for (a) Position 1 (b) Position 2 (c) Position 3

When a differential pair is inserted between transmitter and receiver there will be an insertion loss of -1.2dB/in for three positions. Input impedance varies from 80 ohms to 100 ohms for three positions.

Since there is no fiber weave effect on transmission lines for position 3 further analyses are continued on position 1 and position 2.

4.2.3 Effect of Phase difference and insertion loss on BER counter area

BER contour depends on phase difference. From phase difference plots shown in Figure 46(d), 47(d) we can see peaks for different angle of rotation. A peak value of 300-350 degrees phase difference occurs and it is repetitive as the length increases. Simulations were performed from 0GHz to 50GHz, S-parameters are extracted and inserted 4-port network model in ADS to perform signal integrity analysis on BER contour area.   Values of BER contour area for position 1 with respect to phase difference at 14GHz for each angle of rotation is given in Table 6.

BER area (V-ps)	Phase difference (deg)	Insertion loss (dB)
4.985	2.598	-0.1573
6.353	3.494	-3.208
5.515	5.391	-4.536
5.643	2.809	-6.186
5.624	12.067	-7.5
5.024	10.815	-9.806
1.4258	15.44	-11.5
0.962	43.418	-15.2
0.6578	333.248	-13.603
0.2247	330.814	-15.5

(a) 0 degrees

BER Area (V-ps)	Phase difference (deg)	Insertion loss (dB)
4.963	2.938	-1.484
5.047	6.151	-2.991
5.73	9.245	-4.39
5.674	12.859	-5.9
4.105	16.737	-7.336
4.8336	22.251	-11.834
1.4537	24.702	-11.454
0.9689	44.256	-15.414
0.6785	328.592	-13.38
0.21	335.804	-14.949

(b) 10 degrees

BER Area (V-ps)	Phase difference (deg)	Insertion loss (dB)
5.002	2.3	-1.7
5.23	6.392	-3.148
5.375	9.845	-4.7
5.835	12.647	-6.112

5.549	16.524	-7.742
4.7	24.298	-12.2
1.5	29.624	-11.31
0.987	42.719	-15.752
0.66	328.807	-13.721
0.2055	335.223	-15.85

(c) 20 degrees

BER Area (V-ps)	Phase difference (deg)	Insertion loss (dB)
5.033	2.390	-1.471
5.781	6.479	-2.961
5.324	9.931	-4.588
5.626	12.739	-5.98
5.807	16.605	-7.5
4.68823	18.396	-11.96
1.484	19.963	-11.29
1	21.542	-13.12
0.66	328.730	-13.4
0.206	335.317	-15.04

(d) 30 degrees

BER Area (V-ps)	Phase difference (deg)	Insertion loss (dB)
5.084	2.796	-1.481
6.32	6.898	-3
5.947	9.245	-4.4
6.277	13.606	-6
5.869	17.464	-7.5
5.9681	16.228	-9.5
1.58673	20.703	-11
1.1	26.285	-13
0.6238	327.862	-13.5
0.132	336.183	-14.981

(e) 45 degrees

Table 6. Values of BER contour at (a) 0 degrees (b) 10 degrees (c) 20 degrees (d) 30 degrees (e) 45

degrees at position 1.

Values of BER contour area for position 2 with respect to phase difference at 14GHz for each

angle of rotation is given in Table 7.

BER area (deg)	Phase difference (deg)	Insertion loss (dB)
5.045	2.938	-1.484
5.82	6.841	-2.984
5.947	9.245	-4.39
6	14.638	-5.873
4.054	28.391	-8.318
5.286	34.022	-12.135
1.349	32.473	-12.215
0.6	70.414	-15.79
0.4769	316.953	-14.44
0.4	347.021	-16.2

(a) 0 degrees

BER Area (V-ps)	Phase difference (deg)	Insertion loss (dB)
5.139	4.623	-1.511
5.254	7.008	-2.978
5.224	11.481	-4.445
6.562	15.319	-5.87
4.243	18.165	-7.356
4.372	32.162	-10.983
1.3	32.626	-12.25
0.7746	60.503	-14.495
0.6628	327.174	-13.38
0.1323	336.829	-14.97

(b) 10 degrees

BER Area (V-ps)	Phase difference (deg)	Insertion loss (dB)
4.695	4.238	-1.745
5.128	6.829	-3.082
5.174	11.283	-4.55
5.73	15.113	-5.909
4.074	17.967	-7.416
4.161	32.355	-10.743
1.244	61.032	-14.529
0.7736	60.232	-14.487
0.6427	327.369	-13.47
0.1344	336.654	-15.112

(c) 20 degrees

BER Area (V-ps)	Phase difference (deg)	Insertion loss (dB)
4.866	4.250	-1.544
6	6.652	-2.947
5.855	10.563	-4.395
6.102	13.362	-5.851
4.066	17.729	-7.309
6.328	21.290	-8.829
1.401	29.005	-10.866
0.8045	60.449	-14.395
0.65	328.116	-13.324
0.2022	335.929	-14.912

(d) 30 degree

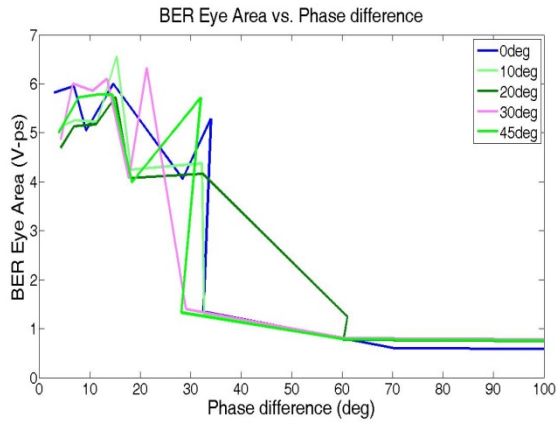| BER Area (V-ps)	Phase difference (deg)	Insertion loss (dB)
5	3.848	-1.488
5.72	7.740	-2.952
5.779	11.657	-4.397
5.774	14.449	-5.852
3.99	18.325	-7.31
5.713	31.968	-11.331
1.327	28.098	-10.903
0.7829	60.545	-14.443
0.6302	324.022	-13.313
0.1899	337.012	-14.898

(e) 45 degrees

Table 7. Values of BER contour at (a) 0 degrees (b) 10 degrees (c) 20 degrees (d) 30 degrees (e) 45

degrees at position 2.

A graph is plotted between BER contour Area and phase difference (peak values of 300-350 degrees) as shown in Figure 54.
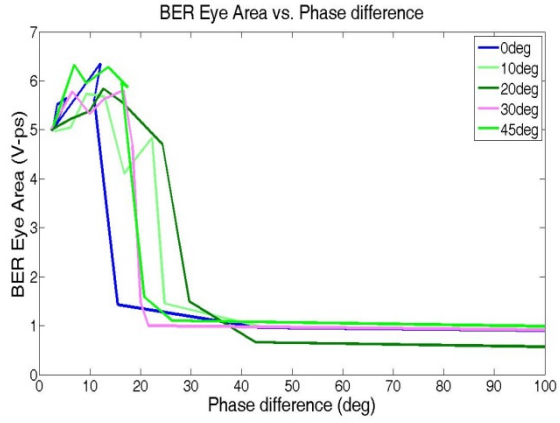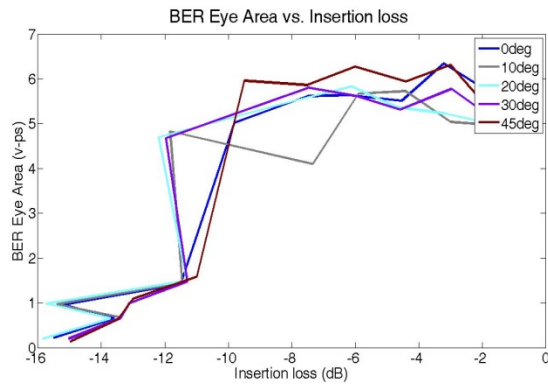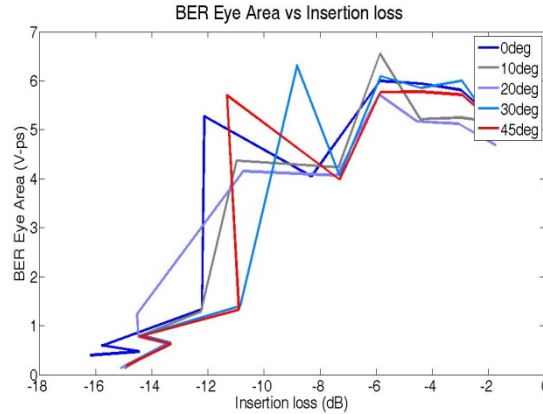
(a) position 1

(b) position 2

Figure 54. BER contour area vs. phase difference for (a) Position 1 (b) Position 2

BER contour also depends on the insertion loss. A graph is plotted between BER contour area and insertion loss shown in Figure 55.

(a) Position 1

(b) Position 2

Figure 55. BER contour area vs. Insertion loss for (a) Position 1 (b) Position 2

For position 1

Phase difference of 25 degrees at 14GHz and insertion loss of -10dB is tolerated beyond which BER contour area drops off to 20% of the maximum value.

For position 2

Phase difference of 30 degrees at 14GHZ and insertion loss of -11dB is tolerated beyond which BER contour area drops off to 20% of the maximum value.

4.2.4 Tight weaves

As discussed in chapter 3.4 use of tight weave will reduce fiber weave effects on differential pair. This can be explained with an example. 7628 laminate weave is considered.

Specifications for 7628 laminate weave given by manufacturers are[23]

- Number of fiber: 17.3X12.2/cm2

- Cloth thickness: 172.72μm

- Fiber diameter: 9μm

- fc150 fibers per bundle

After calculations

- Pitch =44.034 mils

- Radius =17.557mils.

85

A design with above specifications is designed in HFSS as shown in Figure 56
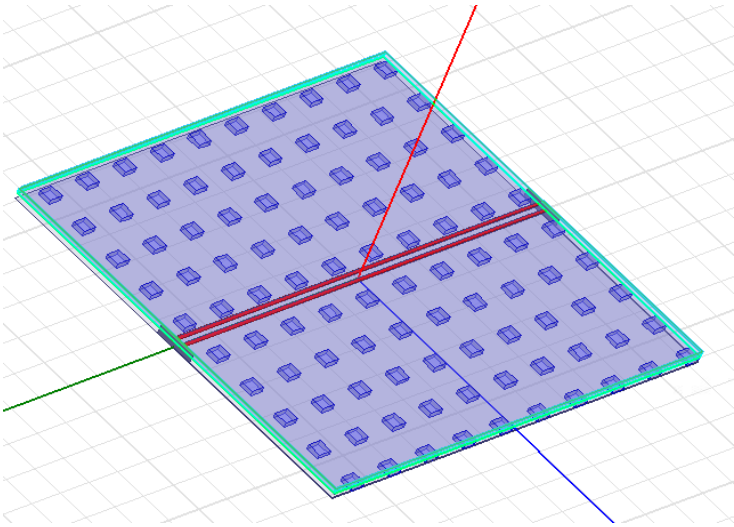
Figure 56. 7628 laminate weave design in HFSS

The dimensions of the design is similar to the one used for 1078 spread weave design. Similar to 1078 spread weave three possibilities arises with respect to position of the transmission lines shown in Figure 56.

(a) Position 1
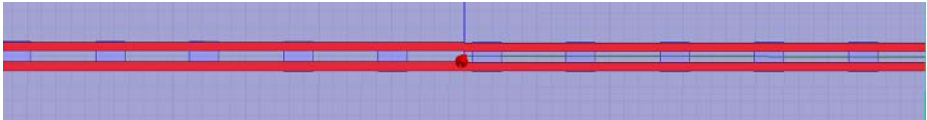
(b) Position 2
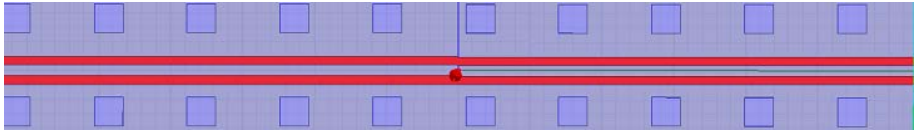
(c) Position 3.

Figure 57. (a) Position 1 (b) Position 2 (c) position 3 for 7628 laminate weave

Simulations were performed from 0GHz to 50GHz and differential to differential return loss, differential to differential insertion loss and differential to common mode conversion loss for position 1

86

are shown in Figure 58.
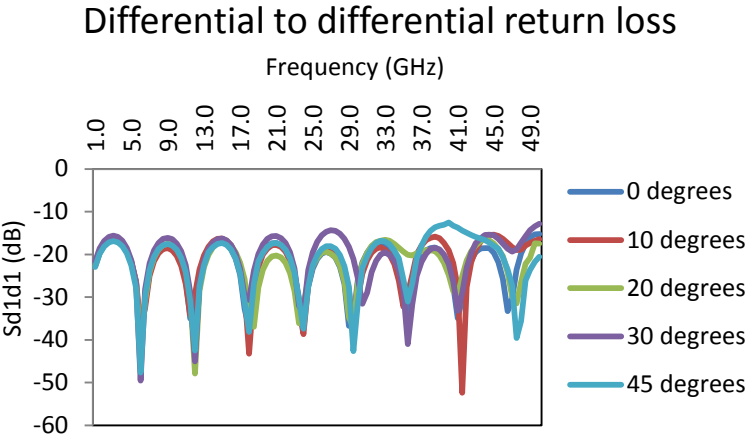
Differential to differential return loss

(a) Differential to differential insertion loss

Differential to differential insertion loss

(b) Differential to differential insertion loss

Differential to common mode conversion

(c) Differential to common mode conversion loss

Phase difference

(d) Phase difference

Figure 58. (a) Differential to differential return loss (b) Differential to differential insertion loss

(c) Differential to common mode conversion loss (d) Phase difference for position 1.

Differential to differential return loss, differential to differential insertion loss and differential to common mode conversion loss for position 2 are shown in Figure 59.

Differential to differential return loss

Frequency (GHz)

(a) Differential to differential return loss

Differential to differential insertion loss

Frequency (GHz)

(b) Differential to differential insertion loss

Differential to common mode conversion

(c) Differential to common mode conversion loss.
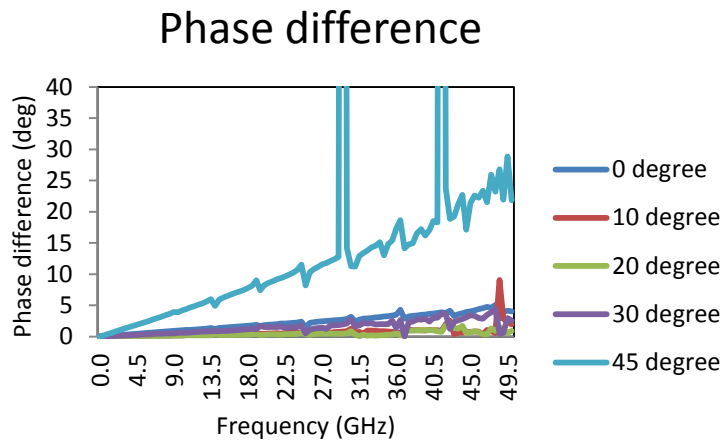
Phase difference

(d) Phase difference

Figure 59. (a) Differential to differential return loss (b) Differential to differential insertion loss

(c) Differential to common mode conversion loss (d) Phase difference for position 2.

Differential to differential return loss, differential to differential insertion loss and differential to
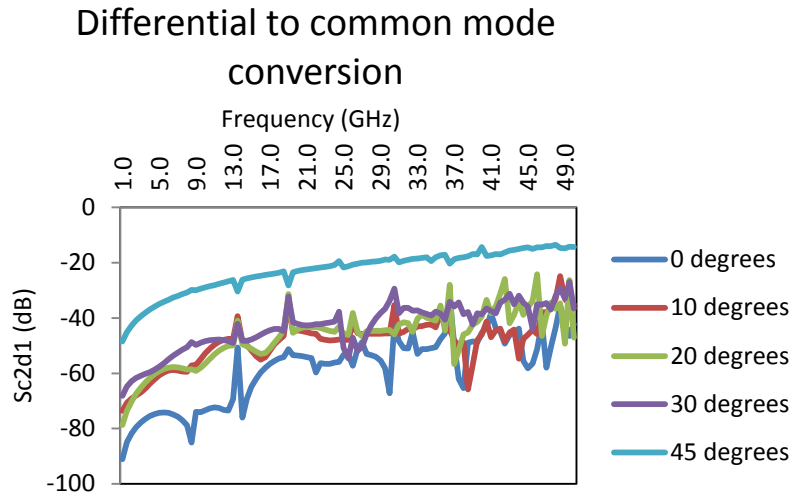
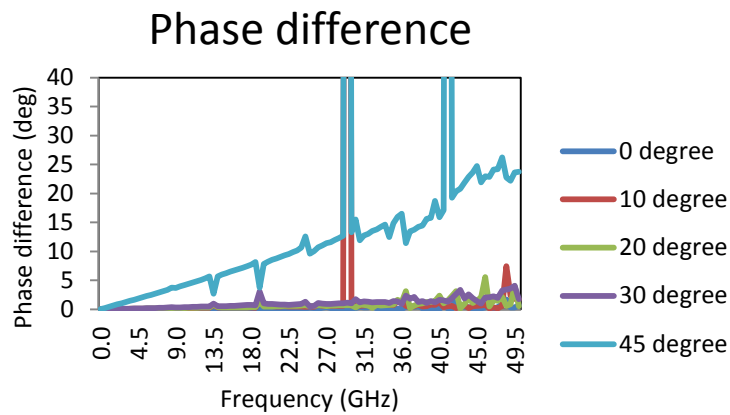common mode conversion loss for position 3 are shown in Figure 60.

Differential to differential return loss
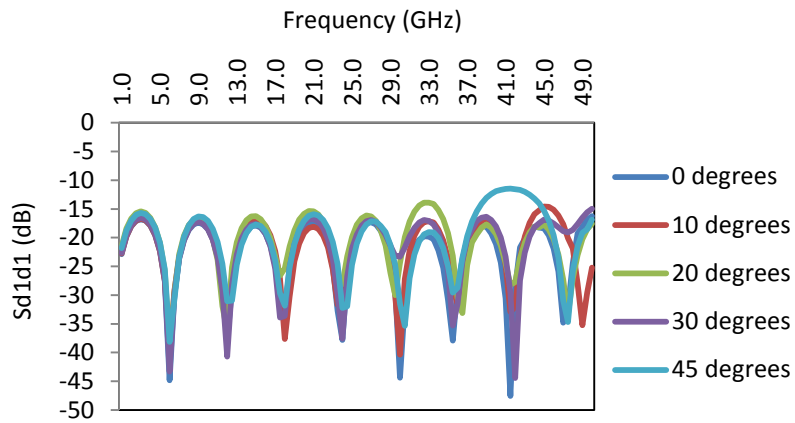
(a) Differential to differential return loss

Differential to differential insertion loss

(b) Differential to differential insertion loss

91

Differential to common mode conversion

Frequency (GHz)
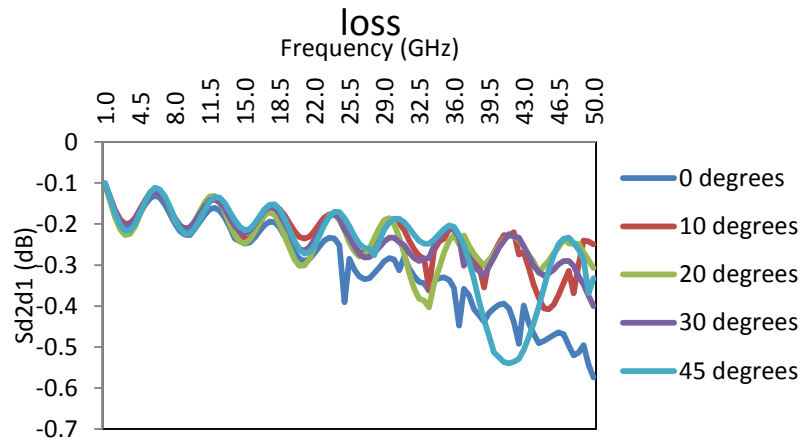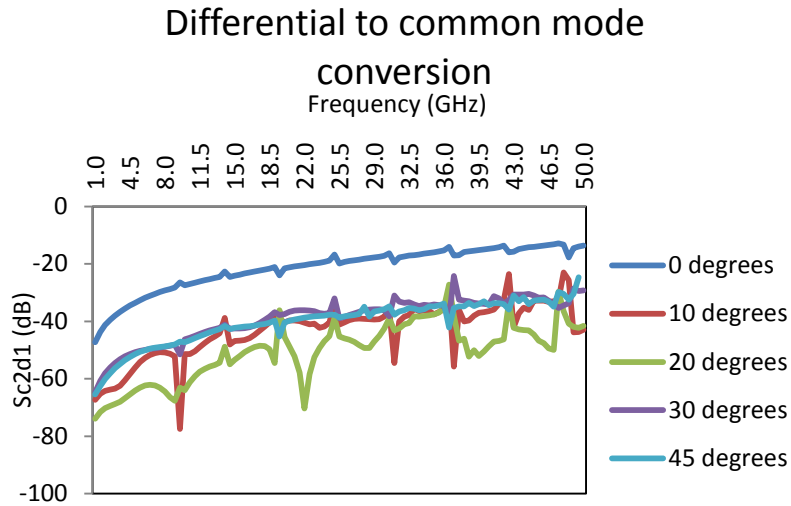
(c) Differential to common mode conversion loss.
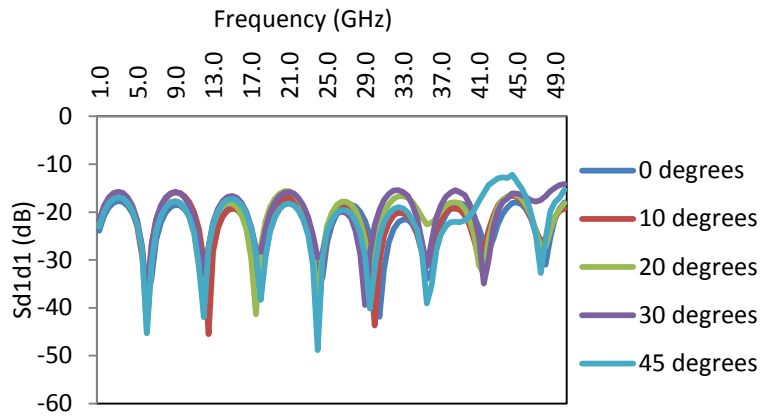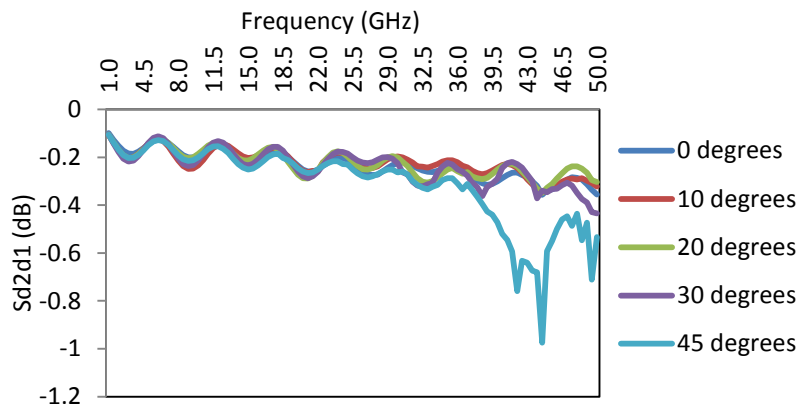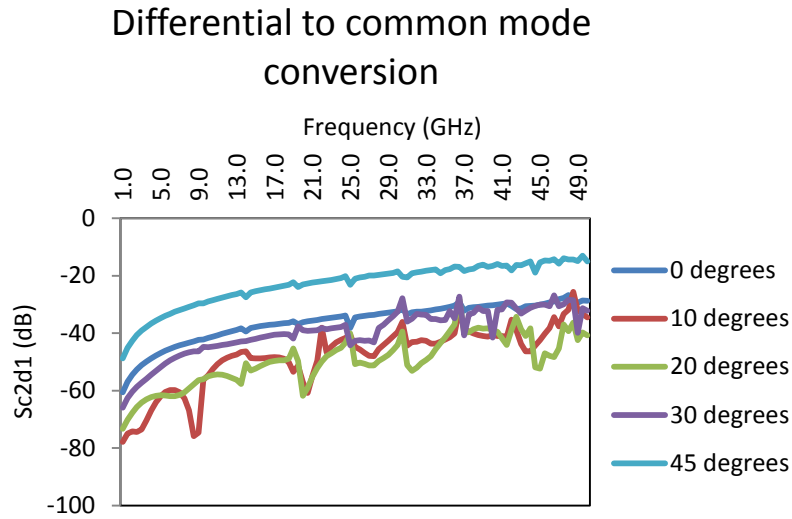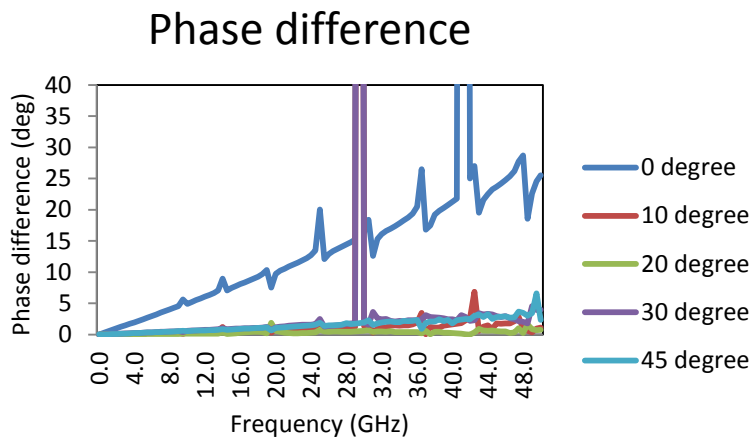
Phase difference

(d) Phase difference

Figure 60. (a) Differential to differential return loss (b) Differential to differential insertion loss

(c) Differential to common mode conversion loss (d) Phase difference for position 3.

Peaks in phase angle plots refer to phase difference of 350 degrees between the differential pair. In order to look at the effect of anisotropic at lower phase difference, graph is limited to lower value.

For position 1 and Position 2

At 20 degrees angle of rotation differential to differential return loss is less than -15dB and

differential to differential insertion loss is -0.4dB. Differential to common mode conversion loss is less than -40dB and phase difference is close to zero degrees between the differential pair.

For position 3

Considerable phase difference exists at zero degree angle of rotation. Since one of the transmission lines is on fiber and another is on pores filled with resin there exist phase difference between the pair and as we rotate transmission lines from zero degree to 45 degree we can see improvement in phase difference.

At 20 degrees angle of rotation differential to differential return loss is less than -15dB and differential to differential insertion loss is -0.4dB. Differential to common mode conversion loss is less than -40dB and phase difference is close to zero degrees between the differential pair.

S-parameters are extracted and inserted into a 4-port network model in ADS. Equalization techniques are applied at the receiver and values for height, width and area of BER contour are tabulated in Table 8 for three positions.

Angle of rotation	Without optimization			With optimization		
	Height (V)	Width (ps)	Area (V-ps)	Height (V)	Width (ps)	Area (V-ps)
0	0.224	8.961	2.00	0.408	11.47	4.681
10	0.219	10.93	2.396	0.371	11.27	4.580
20	0.251	10.93	2.747	0.417	12.37	5.163
30	0.270	10.93	2.948	0.394	12.37	4.875
45	0.197	1.97	0.388	0.389	12.54	4.884

(a) Position 1

Angle of rotation	Without optimization			With optimization		
	Height (V)	Width (ps)	Area (V-ps)	Height (V)	Width (ps)	Area (V-ps)
0	0.202	13.62	2.757	0.420	11.29	4.746
10	0.247	10.04	2.477	0.416	11.65	4.850
20	0.280	11.29	3.158	0.419	14.52	6.075
30	0.185	12.37	2.291	0.435	10.57	4.595
45	0.262	11.29	2.964	0.409	11.83	4.842

(b) Position 2

	Without optimization			With optimization		
Angle of rotation	Height (V)	Width (ps)	Area (V-ps)	Height (V)	Width (ps)	Area (V-ps)
0	0.228	12.37	2.815	0.423	10.93	4.62
10	0.173	12.01	2.076	0.416	12.9	5.369
20	0.338	24.37	8.244	0.338	24.37	8.244
30	0.343	29.03	9.9959	0.343	29.03	9.9959
45	0.173	9.857	1.706	0.415	12.9	5.36

(c) Position 3

Table 8. BER contour values for (a) Position 1 (b) Position 2 (c) Position 3

Corresponding plots are shown in Figure 61

(a) Position 1

(b) Position 2

94

BER Eye Area vs Angle of rotation

(c) Position 3

Figure 61. BER Eye area vs. angle of rotation for (a) Position 1 (b) Position 2 (c) position3.

 For Position 1 and Position 2

   Maximum area can be obtained at 20 degree angle of rotation.

For Position 3

   Maximum area can be obtained at 30 degree angle of rotation.

4.3 Differential skew in isotropic substrates.

   As mentioned in chapter 2.5.9.2 one of the common sources for differential skew in isotropic substrates is unequal length of transmission lines. Several factors affect the electrical length between the transmission lines. Steps should be taken to make sure transmission lines are of equal length.

   Simple model is designed in ADS and a piece of transmission line is added to one of the differential pair as shown in Figure 62. The length of the transmission line is increased in steps of 15 mils to observe phase mismatch between the differential pair. The values of Height, width and Area of BER contour with respect to length of transmission line is given in Table 9.

Figure 62. Simulation for phase mismatch between the differential pair

Length (mils)	Height (V)	Width (ps)	Area (V-ps)
0.1	0.375	12.01	4.506
5	0.374	12.19	4.55
10	0.342	14.16	4.846
15	0.383	12.19	4.666
30	0.392	14.7	5.764
45	0.377	12.37	4.661
60	0.374	12.01	4.493
75	0.368	12.19	4.486
90	0.343	12.72	4.366
105	0.322	12.54	4.037
120	0.289	8.244	2.379
135	0.266	7.885	2.095
150	0.252	8.065	2.034
160	0.196	6.81	1.333
170	0.034	2.867	0.9657
175	0.08	4.839	0.3877

Table 9. Height width and area of BER contour with respect to length.

Phase angle plot and phase difference plots for length of 175 mils is shown in Figure 63.

(a) Phase angle plot

96
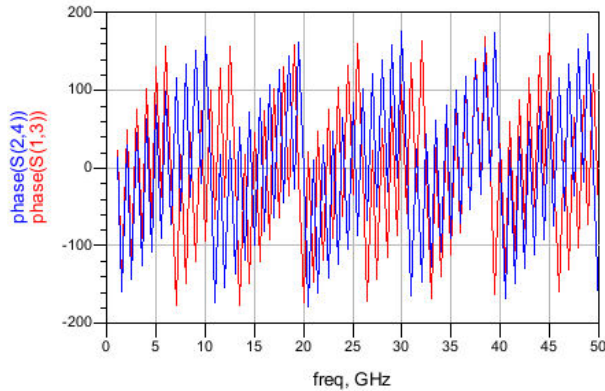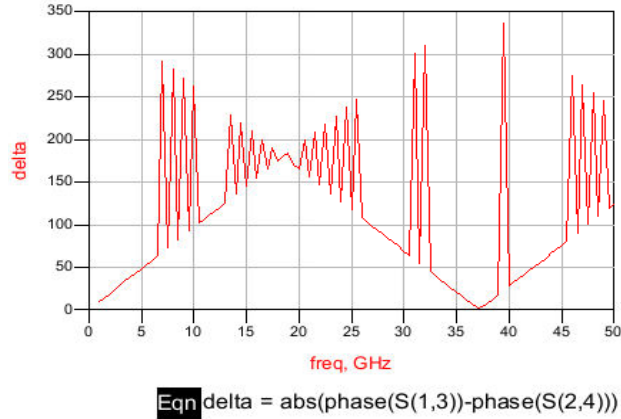
(b) Phase difference plot

Figure 63. (a) Phase angle plot (b) Phase difference plot for 175 mils.

A graph is plotted between BER contour Area and length of the transmission line added to one of

the differential pair shown in Figure 64.
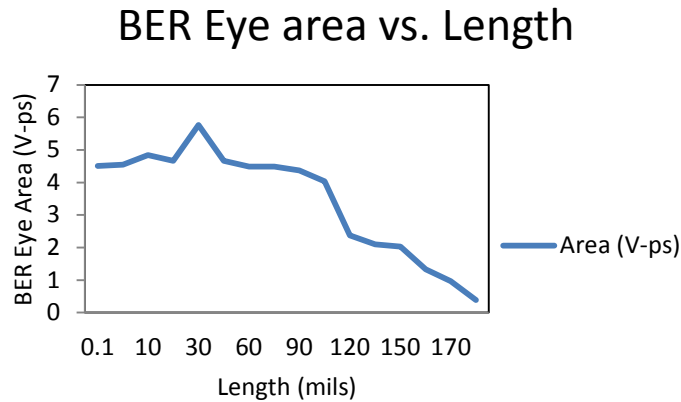
Figure 64. BER contour area vs. length

From Figure 64 maximum length of 150 mils is added beyond which BER contour area will be less than

20% of the maximum value.

Solution to the differential skew in anisotropic substrate is routing of the transmission lines.

97

4.3.1 Routing

There can be many factors for unequal length between the differential pair one of them is explained below.

If there is a defect on PCB board and one of the differential pair is running over the defect steps should be taken to design a different route to the transmission line with multiple bends such that it avoids the defect as well as the electrical length between the differential pair remains same as shown in Figure 65.
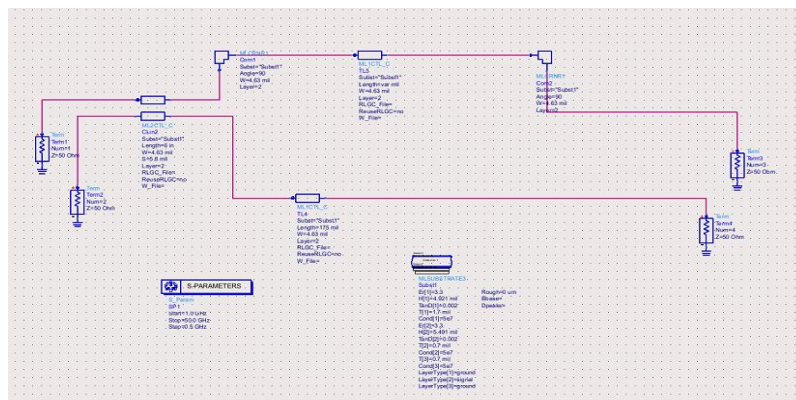
Figure 65. Routing of one of the transmission line with multiple bends

In figure 65 a length of 175 mils is added to one of the transmission lines. Routing is designed for another transmission line with 90 degree bends which accounts for 12 mils of length and a piece of 163mils is added to compensate the mismatch. Phase angle plot and phase difference for Figure 65 is shown in Figure 66.

(a) Phase angle plot

Eqn delta = abs(phase(S(1,3))-phase(S(2,4)))
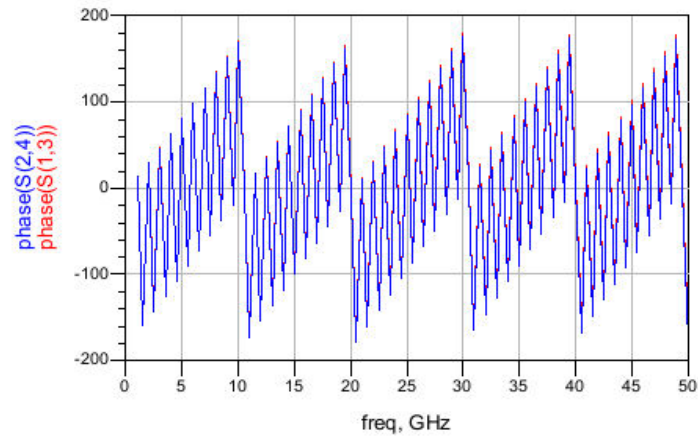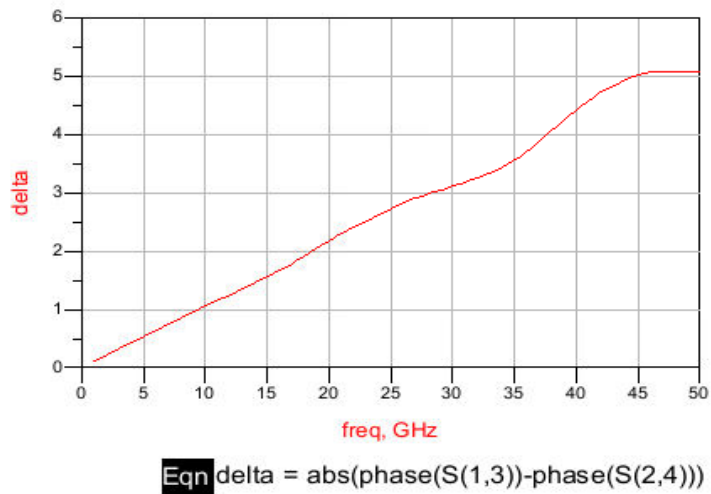
(b) Phase difference plot

Figure 66. (a) Phase angle plot (b) Phase difference plot for routing design

As we are looking at a phase mismatch for a length of 175 mils, mixed mode S-parameters are studied. Graphs for differential to differential return loss, Differential to differential insertion loss and differential to common mode conversion loss are given in Figure 67.

Differential to differential return loss
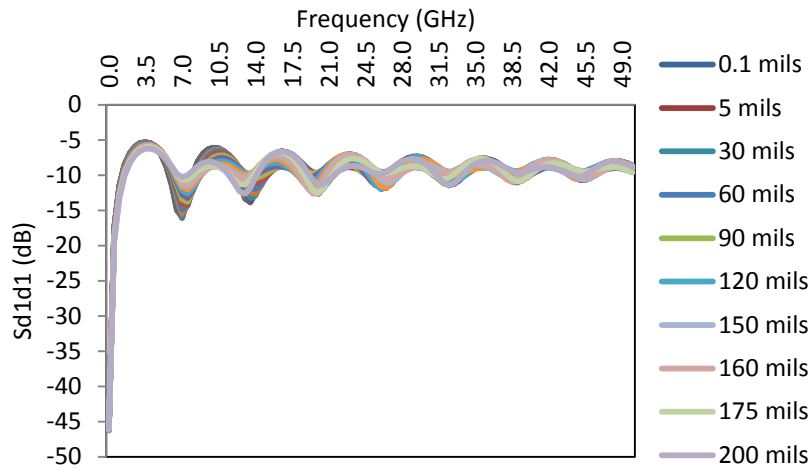
(a) Differential to differential return loss.

Differential to differential insertion loss
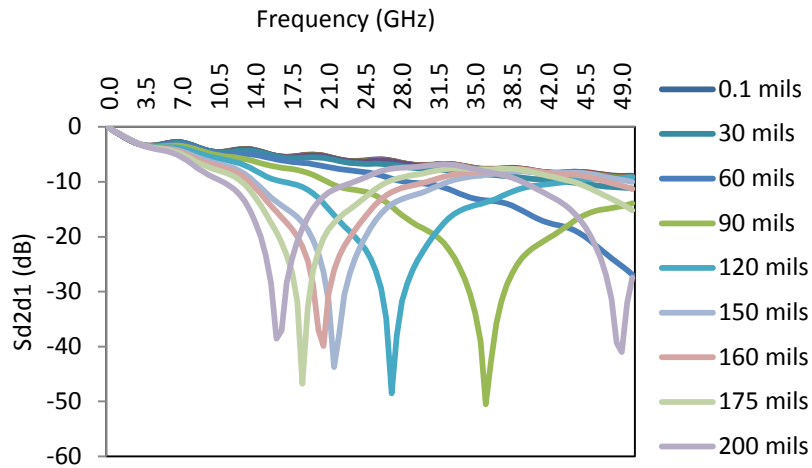
(b) Differential to differential insertion loss

Differential to common mode conversion
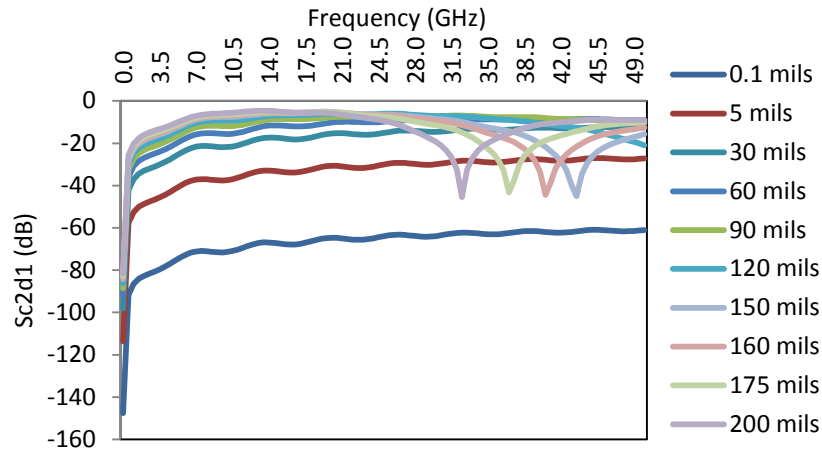
(c) Differential to common mode conversion loss.

Figure 67. (a) Differential to differential return loss (b) Differential to differential insertion loss (c) Differential to common mode conversion loss.

From Figure 67 (a) differential to differential return loss is below -5dB for a phase mismatch of 200mils. For 0.1mil to 200mils length of line return loss varies from -10dB to -5dB. For 0.1mils phase mismatch differential to differential insertion loss is close to -6dB and as the length increases insertion loss decreases to -40 dB for 200mils. Differential to common mode conversion loss is below -40dB for 0.1in and as the length increases to 200 mils conversion loss increases to -5dB.

If we limit the insertion loss to -25dB and mode conversion loss to -15dB then a phase mismatch of 60mils is tolerated between the differential pair.

5. Conclusion and Future work

Transmission lines on Printed Circuit Boards (PCBs), such as stripline, microstrip or co-planar waveguide connecting high speed transmitters and receivers undergo non ideal transmission properties due to anisotropic dielectric properties of PCBs. Printed circuit boards are made up of two materials fiber and resin. Fiber and resin have different dielectric constant and signals propagating through the transmission lines travel with different speeds and loss in these two materials. At low speeds ($< $ GHz) signal edge degradation does not pose an issue but as the speed (data rate) increases ($\geq \simeq$GHz) significant edge degradation can result in bit-error-rate issues. Anisotropic properties of PCBs can limit the signal transmission performance of the communication system and, limit the length and length difference of the transmission lines.

In this thesis, a solution was explored to mitigate the effects of anisotropic dielectric properties of PCBs. The performance of differential transmission lines on printed circuit boards, with lines rotated from zero degrees to 90 degrees angle of rotation with respect to underlying PCB fabric weave in order to average out of the anisotropic effects beneath the differential pair. To investigate this solution a model was designed in HFSS and signal integrity analysis was performed using IBIS-AMI models in ADS with equalization techniques applied at the receiver.

We characterize the differential skew between the lines of differential pair along with the dependence on the position of the transmission lines on printed circuit boards. Analyses are performed for three different positions. For low insertion loss, maximum area and minimum differential skew differential pair are rotated to 45 degrees angle of rotation.

For routing purposes line lengths can be extended up to 6in beyond which BER contour area becomes 20% of the maximum value for the cases studied in this work. For maximum length applications line length can be increased to 7in. phase difference and insertion loss has it effects on BER contour area, beyond 30 degrees phase difference at 14GHz and -10dB insertion loss BER Contour area

102

reduces to 20% of the maximum value.

One of the solutions to mitigate the effects of anisotropic dielectric properties of PCBs is the use of spread (or/ tight) weave, to more evenly distribute the fiber fabric within the resin. Specifications of 7628 spread weave are taken from the manufacturers and we have designed a modal in HFSS. Signal integrity analysis was performed at three different positions. For minimum insertion loss, minimum conversion mode loss, 90% of the maximum eye area and minimum skew, transmission lines are rotated at 20 degrees angle of rotation.

Transmission lines in isotropic substrate also experience phase difference and one of the most common sources is unequal length between the differential pair. In this thesis we have shown the effect of phase mismatch on BER contour area. Depending on the applications we can set the guidelines for maximum phase mismatch. For 28gbps data rate and 10^{-13} BER contour, beyond 150 mils of phase mismatch contour area decreases to 20% of the maximum value. For differential to common mode conversion loss to be below -15dB a phase mismatch of 60 mils is tolerated between the differential pair.

Results shown in this thesis are based on simulations. Measurements should be done to verify the simulation results and used to refine the models. These measurements can be done at the board level with probed or connectorized hardware. Alternatively, measurements can be performed using assembled boards with chips with functional transceivers running at the desired data rates.

High-speed signaling data rates keep increasing and new problems start occurring as these rates increase. Therefore, further work has to be done to determine new limiting factors at higher data rates. One of these factors is length of the transmission lines in anisotropic substrates.

In this thesis, simulations are performed on a single differential pair of transmission lines. As we shift our analysis to complex structures, multiple pairs of transmission lines are routed from transmitter and receiver and one of the important factors to be considered is coupling or crosstalk between the differential pairs. At higher data rates, not only immediate neighboring signals but a neighborhood of signals needs to be analyzed for coupling effects. Simulations should be performed

considering coupling effects since BER contour area is significantly impacted by this jitter due to coupling.

6. References

[1] The Basics of Signal integrity, Part I, *Transmission line effects, Altera Corporation.*

[2] http://upload.wikimedia.org/wikipedia/commons/b/be/RZcode.png

[3] http://upload.wikimedia.org/wikipedia/commons/5/55/NRZcode.png

[4] Stephen Kempainen. Low-Voltage Differential Signaling (LVDS). *Altera Co-operation,2002.*

[5] Eric Bogatin, Mike Resso, Steve Corey. "Practical Characterization and Analysis of Lossy transmission Lines" *High-Performance System Design Conference, Agilent technologies 5988-6500EN, DesignCon 2001.*

[6] Star-Hspice Manual. "Understanding the Transmission Line Theory"; *University of California, Irvine; Electrical and computer engineering, 2001.*

[7] Walt Kester. "Tips about PCB design: Part 2 - Single-card grounding for multicard systems" ; *Embedded cracking the code to systems development, 2008.*

[8] Symmetric Stripline Analysis/Synthesis calculator, *Dan McMahill,CGI,2001-2009.*

[9] Brian C. Wadell." Introduction to Common Printed Circuit Transmission Lines" . *Artech House, Maxim Integrated Products. ISBN 0-89006-436-9,2003.*

[10] Thomas Kugelstadt. "SIGNAL CHAIN BASICS (Part 29): Digital interfaces - Single-ended versus differential interfaces". *Planet Analog, 2009.*

[11] http://en.wikipedia.org/wiki/Scattering_parameters

[12] David M. Pozar, 4th edition "Microwave Engineering", *Wiley publications*, ISBN *:9780470631553, 2012.*

[13] Gary Breed." Analyzing Signals Using the Eye Diagram". *High Frequency Electronics,2005.*

[14] Application Note. " Bridging the Gap Between BER and Eye Diagrams — A BER Contour Tutorial". *Tektronix, Inc©, 2010*.

[15] Jason Howie. "Improved-interactive length tuning for differential pairs". *Altium Documentation, 2012.*

[16] M. Park, J. Bulzacchelli, D. Friedman. "A 7 Gb/s 9.3 mW 2-tap current-integrating DFE receiver," *in IEEE ISSCC Dig. Tech. Papers, Feb. 2007, pp. 230–231.*

[17] Garth Sundberg." Grasp The Meaning Of Mixed-Mode S-Parameters". *Maxim Integrated Products, 2001.*

[18] Allan Huynh, Magnus Karlsson, Shaofang Gong." Mixed-Mode S-Parameters and Conversion Techniques". *Advanced Microwave Circuits and Systems, ISBN 978-953-307-087-2, 2010.*

[19] David E. Bockelman, William R. Eisenstadt. "Combined Differential and Common-Mode Scattering Parameters: Theory and Simulation," *IEEE Trans. On MTT, vol. 43, pp.1530–1539, 1995.*

[20] Channel Simulation for AMI, *Advance Design Systems, Agilent technologies© 2011.*

[21] Scott McMorrow, Chris Heard. "The impact of PCB laminate weave on electrical performance of differential signaling at Multi-Gigabit data rates", *Designcon2005.*

[22] Application note;, " PCB Dielectric Material Selection and Fiber Weave Effect on High-Speed Channel Routing", *Altera Corporation©, 2011.*

[23] Eric N. Brown, N.R. Sottos," Thermoelastic Properties of Plain Weave Composites for Multilayer Circuit Board Applications", *Department of Theoretical and Applied Mechanics,University of Illinois at Urbana-Champaign,1995.*

[24] J. F. Bulzacchelli, et al. "A 10-Gb/s 5-Tap DFE/4-Tap FFE Transceiver in 90-nm CMOS Technology", *IEEE Journal of Solid-State Circuits, Vol. 41, No. 12, Dec. 2006, page 2885~2900.*

[25] Digital Systems Engineering, W. Dally and J. Poulton, Cambridge University Press, 1998.

[26]   R. Payne et al,"A 6.25-Gb/s Binary Transceiver in 0.13-um CMOS for Serial Data Transmission Across High Loss Legacy Backplane Channels," *JSSC, vol. 40, no. 12, Dec.2005, pp. 2646-2657.*

[27]   Rick Hartley, " The Truth about Differential Pairs in High Speed PCBs", *L-3 Avionics Systems, Inc,2009.*